Alma Mater Studiorum · University of Bologna

School of Science
Department of Physics and Astronomy
Master Degree in Physics

Early matter domination from a dark photon at colliders

Supervisor:
Prof. Filippo Sala

Submitted by:
Carlos García Sánchez

Academic Year 2023/2024

Abstract

In this thesis we study the detectability at colliders of long-lived particles (LLP) which, at the early stages of the Universe, dominate its energy density and decay injecting entropy in the thermal bath, thus diluting early Universe relics. Such periods of early matter domination are predicted in many models, and allow for example to obtain thermal dark matter heavier than 100 TeV. We compute the dilution factor induced by a generic LLP as a function of its decay length and mass. Then we apply our results to the well known dark photon model. After re-deriving known dark photon properties, we demonstrate that forthcoming LLP detectors such as CODEX-b, ANUBIS and MATHUSLA (ordered from realised in the next few years to maybe realizable in the future) could test the parameter space where a dark photon, produced from heavier dark matter annihilations, induces a period of early matter domination with sizeable dilution of pre-existing relics.

Contents

1 Introduction

From the end of reheating after inflation down to a temperarture of $T =$ few eV corresponding to a time of $t = 10^{12}$ s (radiation-matter equality) in the history of our Universe, the Standard Model (SM) predicts that the energy budget of the Universe is dominated by radiation (see for example subsection 2.4.6 and section 2.5 in [1]). However, the SM fails in explaining several observational and experimental results (dark matter, neutrino oscillations, baryon asymmetry...), requiring the existence of physics beyond the SM (BSM) that could alter radiation domination at temperatures larger than an eV.

Dark Matter (DM), an unknown form of matter that dominates the gravitational behaviour of visible matter[1] (matter that can interact with light) in galaxies (galaxy rotation curves with the very ground breaking article of Rubin et al. [3]), in galaxy clusters (coma cluster, Zwicky [4] or the bullet cluster, e.g. Clowe et al. [5]) and that is a very plausible responsible of the Large Scale Structure (LSS) of our Universe (Cold Dark Matter and LSS simulations, see section 1.3.2 of [2] and Cosmic Microwave Background acoustic peaks[2], see section 1.3.3 of [2]), is thought to constitute around the 25% of matter content of the Universe leaving only a 5% to baryonic matter (see section 2.4 of [1] and [6] for a historical review of Dark Matter).

In the 2000s a very reasonable candidate for DM were the WIMPs (Weakly Interacting Massive Particles) with masses $M_{\rm DM}$ between the GeV and TeV range, and an interaction strength α with the SM of the same order of the Weak one. These particles are in equilibrium with the SM bath in the early Universe and explain in a natural way today's DM abundance via the thermal freeze-out mechanism. Any particle in equilibrium with the SM bath is said to 'freeze-out' from it when the rate of its number changing interactions, $\Gamma = n\langle\sigma v\rangle$ with n its number density and $\langle\sigma v\rangle$ its averaged annihilation cross-section times relative velocity, falls below the Hubble rate with which the Universe expands, $H = \sqrt{\rho/3}/M_{\rm Pl}$ with ρ the total energy density of the Universe and $M_{\rm Pl} \simeq 2.4 \times 10^{18}$ GeV the reduced Planck mass. The present number density of neutrinos is for example set via thermal freeze-out, which happens when they are relativistic in the early Universe. If a particle instead freezes out while it is non-relativistic, one can show (see e.g. section 4.1.2 of [2]) that it reproduces the measured DM relic abundance if $\langle\sigma v\rangle \simeq 3 \times 10^{-26}{\rm cm}^3/{\rm s} \simeq 1/(20\ {\rm TeV})^2$, where in the last equality we have used natural units $\hbar = c = 1$. That value is almost independent of the particle mass.

[1] It is non-interacting, meaning the interactions among DM particles or with SM content are negligible (except for gravitational interaction, that DM certainly possesses). In addition, to explain the Large Scale Structure of the Universe it must be non-relativistic (CDM) at the radiation-matter equality in order to cluster first and form later the large structure of the Universe (see section 1.3 of [2] for a complete description of DM at cosmological scales).

[2] The position of the acoustic peaks in the CMB depend on the DM density and their amplitude on the relative amount of DM w.r.t. ordinary matter. So the precise measurement of these peaks by the Planck collaboration and the consistence with the ΛCDM cosmological model represents the strongest evidence of DM.

For a WIMP one has $\langle \sigma v \rangle \approx \alpha^2 / M_{\rm DM}^2$, implying that if one demands it to constitute DM then a weak coupling implies a mass $M_{\rm DM}$ roughly at the weak scale. Since physics BSM was predicted at the weak scale independently by natural solutions of the hierarchy problem, this coincidence was dubbed as "WIMP miracle", see e.g. [7] for a review of supersymmetry and WIMPs. The Large Hadron Collider (LHC) however has found no evidence for the natural BSM physics that should have solved the hierarchy problem, see e.g. [8], weakening the theory motivation for WIMPs as DM. In addition direct and indirect DM detection experiments, built to find WIMPs, have so far not discovered any. While the search is still in progress and WIMPs are not excluded as a DM candidate, the theory community has shifted its attention to other ranges of DM mass.

The energy above a TeV is still not in trouble with experiments and thus it is easier to accommodate hidden sectors (also called dark sectors) [3] at such higher energies. With the advent of new experiments (e.g. new colliders such as the Future Circular Collider [9]) we will have the opportunity to explore nature at much higher ranges. At scales larger than tens of TeV, however, thermal DM would violate S-matrix's unitarity i.e. $SS^\dagger \neq 1$ for heavy thermal DM. The unitary bound on the DM mass was first noted and computed by Kim Griest and Marc Kaminkowsky back in 1990 [10], recent calculations (see e.g. [11]) imply that DM should be lighter than about 100 TeV. This bound is obtained by combining unitarity (imposed by $SS^\dagger = 1$) of non-relativistic cross section partial waves with a simple non-relativistic freeze-out scenario i.e. before freeze-out; the energy budget of the Universe is dominated by radiation, DM and SM are in chemical equilibrium and DM abundance is mainly controlled by 2-2 interactions. The condition $SS^\dagger = 1$ translates in an upper limit on σv upon partial wave expansion, as one can see in figure 1. Still, the unitary bound can be increased if one of the assumptions is not satisfied, as we will see next, opening the door to heavy thermal DM.

As said before, the SM predicts a radiation dominated Universe at its early stage, but with new particle content this could not be the case. Triggered by the existence of a new particle (for example a possible mediator between the dark sector and SM, see e.g. section 2 of [12]), much before the matter-radiation equality for temperatures $T > 5$ MeV [4], there could have been what is called an Early Matter Domination (EMD) epoch (see [14]) that would violate the unitarity bound assumption of a radiation dominated Universe. The actual DM abundance, if we suppose thermal CDM, is predicted to depend inversely on the thermal average $\langle \sigma v \rangle$ (again, see e.g. section 4.1.2 of [2]) i.e. $\Omega_{DM} \propto \frac{1}{\langle \sigma v \rangle}$. As is described in section 2, an EMD epoch can be traduced into a sizeable injection into the SM entropy and a dilution of the DM yield $Y_{DM} = \frac{n_{DM}}{s_{SM}}$ meaning the actual DM

[3] A hidden sector is thought of as a group of gauge symmetries and fields that is connected only by gravity, or by gravity and weakly by some new force, with the observable sector that contains SM particles.

[4] In order to be consistent with Big Bang Nucleosynthesis this EMD epoch must have happened from Big Bang to $t \sim 0.03$ s or $T \sim 5$ MeV in the history of our Universe (bounds computed in [13]) and so we talk about EMD for temperatures $T > 5$ MeV.

abundance depends also on a new factor, $\Omega_{DM} \propto \frac{1}{\langle\sigma v\rangle} \frac{s_{SM}^{before}}{s_{SM}^{after}}$. If the injection is important ($s_{SM}^{after} > s_{SM}^{before}$) then the thermal average of the cross section times the relative velocity of the DM particles, $\langle\sigma v\rangle$, has to decrease to obtain the actual DM abundance. In that case the unitary bound could be increased and heavy thermal DM could be conceived. See figure 1 for a sketch of this situation.

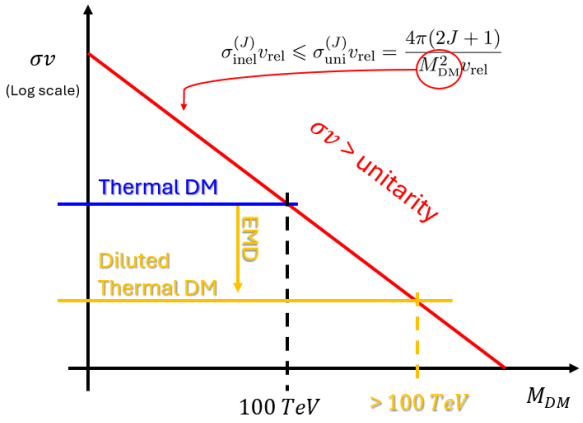

Figure 1: Change in the unitary bound on the DM mass when EMD is realised. It is represented, in logaritmic scale, the cross section times the relative velocity of DM particles vs the DM mass. The red line is the frontier between the unitarity zone and the unitarity violation zone; for values of $\langle\sigma v\rangle$ higher than the unitarity line, violation of unitarity forbids thermal CDM, for lower values unitarity is statisfied. The line has negative slope because the unitarity bound depends inversely on the mass as one can see e.g. in Griest and Kaminkowsky's result [10]. The blue line represents the value of $\langle\sigma v\rangle$ to obtain the actual DM abundance via non-relativistic thermal freeze-out and in light orange are represented the new required $\langle\sigma v\rangle$ and the new unitary bound when EMD is realised.

On the other hand, an EMD epoch would be also important for primordial Gravitational Waves (GWs). These GWs are hypothetically produced during inflation, by cosmic strings and/or by a strong first-order phase transition (see sections on GW in [15] for a complete review of these production mechanisms). As new GWs detectors are coming such as the Einstein Telescope, LISA or Cosmic Explorer, an ancient remnant (Stochastic Gravitational Waves Background, SGWB), arriving from a much more younger Universe than the well-known CMB signal, could be unveiled in the next upcoming years. However, if the production of these GWs happened before an EMD, then the entropy injection would decrease the actual energy density of these GWs. That would mean less chance to see primordial GWs. Nevertheless, if detectors have enough sensitivity to detect them, as the dilution would have happened for a determined GWs'

frequency, a "step" would appear in their frequency and we could learn that dilution happened and at what temperature.

An EMD and the decay into SM radiation of the particles that trigger it can induce a siezable injection to the SM entropy and therefore a dilution of the yield ($Y_x = \frac{n_x}{s_{SM}}$) of any pre-existing specie in general (see subsection 2.3 in [12] or [14]). it is important to remark that the particle that induce EMD is unstable and no longer around in the Universe today, so it cannot be the DM. The two main requirements that this new particle must fulfill in order to cause a sizeable dilution, as described in the introduction of [16], are:

1. It mustn't be in equilibrium with the thermal bath when decaying while having a large number density (e.g. a particle that decouples while relativistic).

2. It has to be non-relativistic when it decays.

If the particle decouples while non-relativistic its yield is exponentially suppressed in $x = m_V/T_{FO}$ and it is difficult for it to dominate the energy density of the Universe. In the case of a particle that is relativistic when decaying we have that the injection of entropy only depends on the yield of the particle when it froze out making it difficult to induce a sizeable entropy injection (see appendix A in [12] for a detailed explanation of these points).

To ensure a sizeable dilution of relic in the early Universe, a particle should have a decay length of a meter or larger (if it is not a very heavy particle), as we will prove in section 2.3. Therefore it is natural to ask whether searches for Long-Lived Particles (LLPs) at colliders could directly test an EMD epoch. However, the SM-LLP couplings necessary to decouple the particle while relativistic give a low decay rate so that their production at the lab is often negligible, as it has been the case of the dark photon (DP), for example. Nevertheless, improving and searching for new ways to find LLP at colliders (experiments CODEX-b [17], ANUBIS [18] or MATHUSLA [19]) can make this problem avoidable (we study this case in section 4).

In this thesis we will re derive the dilution factor via the Simultaneous Decay Approximation in section 2.1 and via numerical integration in section 2.2 to finally correlate it with the decaying particle decay length and mass in section 2.3. Then we will introduce the dark photon minimal model and the Higgs mixed sector in section 3 to prove that a sizeable Higgs to two dark photons decay is possible. Finally, with the latter, we will have the sufficient theoretical support to prove in section 4 that upcoming dectectors CODEX-b [17], ANUBIS [18] and MATHUSLA [19] could test the parameter space of a dark photon that would have induced a period of early matter domination with sizeable dilution of pre-existing relics.

2 Dilution factor derivation

The dilution factor is normally defined as the ratio between the SM entropy density before and after the diluting particle, we will call "V", decays:

$$D_{SM} = \frac{s_{SM}^{after}}{s_{SM}^{before}} \tag{1}$$

The easiest approach to compute it is the one of the Simultaneous Decay Approximation (SDA) where one supposes that the decay of all V particles occurs in an infinitesimal time at Universe's time $t = \tau_V = \Gamma_V^{-1}$. As we will show explicitly, this approximation allows to achieve a result for the dilution factor with the correct parametrical dependence. However, its physical meaning should not be taken seriously. Indeed, the SDA leads to the conclusion that the temperature of the Universe increases as entropy does so (because of the entropy injection due to V's decay). In reality what happens is that at an early time during the EMD epoch the temperature of the Universe starts decreasing as a Universe dominated by matter (decreasing faster than the radiation dominated Universe) but when particles start to decay and entropy is injected the temperature starts to decrease slower than the radiation dominated case until all V particles have decayed (see figure 2 of [12]). Then the Universe recovers the radiation dominated behaviour and its corresponding temperature as if no matter domination had occurred (as far as temperature is concerned) meaning the decay of V particles does not heat up the Universe (a result first obtained by Robert J. Scherrer and Michael S. Turner in 1985 [14]).

A more accurate equation for the dilution factor is obtained numerically integrating Friedmann equation and entropy and energy density expressions (see subsection 2.2 for more details). The expression for the dilution factor we will use for our results is the following:

$$D_{SM} \simeq \left(1 + 0.77\,(g_{SM}^{dec})^{1/3} \left(\frac{m_V f_V}{\sqrt{\Gamma_V M_{Pl}}}\right)^{4/3}\right)^{3/4} \tag{2}$$

Which is the same used in [12] and [16]. In this expression, g_{SM}^{dec} is the SM degrees of freedom at $t = 1/\Gamma_V = \tau_V$ (V refers to the decaying particle), of course, Γ_V is the decay rate, τ_V is the particle's lifetime and m_V is the particle's mass. On the other hand, f_V represents the ratio between the number density of V particles and SM's entropy density (the yield) at freeze-out time i.e.

$$f_V = \frac{n_V^{FO}}{s_{SM}^{FO}} \tag{3}$$

and $M_{Pl} = 1/\sqrt{8\pi G} \simeq 2.4 \times 10^{18}$ GeV. Equation (2) turns out to give really good results for the dilution factor giving an error lower than 10% w.r.t. the full integrated solution

in the relevant zone for our work at (m_V, τ_V) and $(m_{A'}, \varepsilon)$ [5] parameter spaces (see figure 11 on appendix A of [12]).

In this section we will aboard the analytical Simultaneous Decay Approximation and a numerical integration obtaining equation (2).

2.1 Analytical derivation (Simultaneous Decay Approximation)

As we suppose a simultaneous decay of all V particles in this approximation, we don't need to integrate the Friedmann equation. Just with the entropies and energy densities of the Standard Model + V particle before and after the decay we can obtain an expression for the dilution factor of Eq. (1).

The energy densities before and after the decay are, respectively,

$$\rho_b = \left(\frac{\pi^2}{30}\right) g_{SM} \left(T^b_{SM}\right)^4 + m_V f_V \left(\frac{2\pi^2}{45}\right) g_{SM} \left(T^b_{SM}\right)^3, \tag{4a}$$

$$\rho_a = \left(\frac{\pi^2}{30}\right) g_{SM} \left(T^a_{SM}\right)^4 \tag{4b}$$

where suffix "b" means "before" and suffix "a" means "after". Using for the time of the decay $t_{dec} \sim 1/H_{dec}$ and Friedmann's equation (supposing V particles dominate the energy density before the decay) we obtain another important equality:

$$\rho_a = \rho_b = \frac{3M_{Pl}}{8\pi\tau_V^2} \tag{4c}$$

Here we have supposed that V particles are non-relativistic before the decay and $t_{dec} \sim \tau_V$. The energy density before the decay, i.e. ρ_b of Eq. (4a), is constituted by two contributions: the first one, ρ^b_{SM}, is the energy density corresponding to the SM radiation before the decay and the second one, ρ^b_V, is the energy density of the decaying particle V. We will keep that in mind when making approximations in the following.

On the other hand, we have that the SM entropy density before and after the decay has the simple form:

$$s^b_{SM} = \left(\frac{2\pi^2}{45}\right) g_{SM} \left(T^b_{SM}\right)^3, \tag{5a}$$

$$s^a_{SM} = \left(\frac{2\pi^2}{45}\right) g_{SM} \left(T^a_{SM}\right)^3 \tag{5b}$$

In equations (4) and (5) the SM degrees of freedom g_{SM} are evaluated at time $t_{dec} \sim \tau_V = \Gamma_V^{-1}$.

[5] Parameter space for the Dark Photon model, see 3.1 for a brief review.

Now, we want to obtain Eq. (1) and using Eqs (5) we arrive straightforwardly to:

$$D_{SM} = \frac{s_{SM}^{after}}{s_{SM}^{before}} = \left(\frac{T_{SM}^{a}}{T_{SM}^{b}}\right)^{3} \tag{6}$$

Here one can conclude (mistakenly, as mentioned before) that the Universe would be heated up if there's an entropy injection caused by the particle's decay. While this is not the case, as we will show in Sec. 2.2, it still allows to obtain the correct parametrical dependence for the dilution factor. Carrying on with our derivation, using eqs (4) and equating (4b) with (4a) one obtains:

$$\left(T_{SM}^{b}\right)^{4} + \frac{4}{3} m_V f_V \left(T_{SM}^{b}\right)^{3} = \left(T_{SM}^{a}\right)^{4}$$

then the next follows solving for $\left(T_{SM}^{a}/T_{SM}^{b}\right)^{3}$

$$\left(\frac{T_{SM}^{a}}{T_{SM}^{b}}\right)^{3} = \left(1 + \frac{4}{3} m_V f_V \frac{1}{T_{SM}^{b}}\right)^{3/4} \tag{7}$$

At this point we can make use of $\rho_V^b \gg \rho_{SM}^b$ i.e. V particles dominate before the decay (there's an EMD epoch) to obtain T_{SM}^b. Via equations (4a) and (4c) we have:

$$T_{SM}^{b} \approx \left(\frac{135}{16\pi^3}\right)^{1/3} \left(\frac{M_{Pl}}{\tau_V}\right)^{2/3} \frac{1}{g_{SM}^{1/3} (m_V f_V)^{1/3}} \tag{8}$$

Then substituting in Eq. (7) we arrive finally to the dilution factor expression for SDA:

$$D_{SM} \approx \left(1 + 2.06\ g_{SM}^{1/3}\ \left(\frac{m_V f_V}{\sqrt{\Gamma_V M_{Pl}}}\right)^{4/3}\right)^{3/4} \tag{9}$$

This is an approximated result for the dilution factor and it has the same parameter dependence as expression (2), indeed it only differs in the numerical factor which, however, it is 2.68 times larger than the one present in Eq. (2) (in the SDA the dilution is significantly larger than the numerical integration case). Expression (9) gives us a good idea of the behaviour of the dilution factor w.r.t. the particle V's free parameters (mass m_V and decay rate Γ_V) that would be what exprimentalists would be able to measure in colliders.

By making, once again, the matter domination approximation $\rho_V^b \gg \rho_{SM}^b$ at the time of the decay, one obtains the expression (1d) in [14] or expression (25) in [20] [6]:

[6] In reality what one obtains is the numerator (1 in front of expression (25) of [20] was added to make the comparison with radiation domination case) because what is computed in [20] is the dilution factor corresponding to the total entropy of the Universe.

$$D_{SM} \sim 1.72\ g_{SM}^{1/4}\ \frac{m_V f_V}{\sqrt{\Gamma_V M_{Pl}}} \tag{10}$$

This same expression can be obtained as well using equations (8) and (6) and the temperature of the SM bath after V decay; T_{SM}^a [7].

2.2 Numerical integration

In this section we will present the procedure carried on in order to arrive to expression (2). First, we will demonstrate a more general dilution factor expression and the Friedmann's equation for the normalised scale factor (defined in Eq. (23)), in presence of SM radiation and of the V particle that decays into SM radiation (equation (44) at appendix A in [12] or equation (A5) at appendix of Scherrer and Turner's article [14]), as Scherrer and Turner did in [14]. Then, we will show how did we manage to integrate numerically Friedmann's equation and what was the criteria followed in order to finally arrive to Eq. (2).

2.2.1 Obtaining the general dilution factor equation and Friedmann's equation à la Scherrer and Turner

We work under the following usual motivated assumptions:

1. At all times the microscopic entropy of the Universe is dominated by relativistic particles.
2. The decaying particles rapidly thermalise into SM radiation ($\Delta t \ll H^{-1}$).
3. We restrict to Friedmann-Robertson-Walker cosmological models.

The entropy per comoving volume of the Universe can be written as:

$$S(t) = R(t)^3 s(t) \tag{11}$$

where $R(t)$ the scale factor and $s(t)$ is the entropy density. The latter can be expressed as usual:

$$s(t) = \frac{\rho + p}{T} = \frac{2\pi^2 g_*(T(t))}{45}\ T(t)^3 \tag{12}$$

Here $g_*(T(t))$ represents the effective degrees of freedom of all particles (which in our case will consist in the SM at a thermal bath's temperature $T(t)$). ρ and p are the energy density and pressure of particles respectively. To simplify computations we will define

[7] Easily derived by equating eqs (4b) and (4c).

$$a \equiv \frac{2\pi^2 g_*(T(t))}{45} \tag{13}$$

From this we can introduce the new particle that decays into SM radiation. To do so, we define a time t_0 much before the decay of V particles, i.e. $t_0 \ll 1/\Gamma_V$, we suppose V particles are non-relativistic at this time i.e. $T_0 \ll m_V$ and that their abundance is frozen out, i.e. there is no creation nor annihilation of V particles. These are equivalent to the two conditions mentioned in the introduction except for the abundant energy density one that we will use in the next subsection. We can then define

$$f_V \equiv \left(\frac{n_V}{s}\right)\Big|_{T_0} \tag{14}$$

which is the ratio at time t_0 between the number density of V particles and s, the entropy density of the Universe. In other words, f_V is the yield of the particle V at T_0. Then, we can write the V particles' energy density at time t_0, of course non-relativistic

$$\rho_{V0} \equiv m_V \, f_V \, s(T_0) \tag{15}$$

To see what is the effect of this particle in the entropy we need to know its evolution. The evolution of V particles can be described by the Boltzmann's equation of an exponentially decaying particle:

$$\dot{\rho_V} = -3H\rho_V - \Gamma_V \rho_V \tag{16}$$

where the second term of the r.h.s. accounts for the decay effect in the energy density of V. Eq. (16) is easily solved if multiplied by $1/R(t)^3$ and making use of the chain rule $\frac{1}{R^3}\frac{d(R^3\rho_V)}{dt} = \dot{\rho_V} + 3\frac{\dot{R}\rho_V}{R}$:

$$\begin{aligned} \dot{\rho_V} &= \frac{1}{R^3}\frac{d(R^3\rho_V)}{dt} - 3\cancel{\frac{\dot{R}\rho_V}{R}} = -3\cancel{\frac{\dot{R}\rho_V}{R}} - \Gamma_V\rho_V \\ \implies & \frac{d(R^3\rho_V)}{dt} = -\Gamma_V R^3 \rho_V \end{aligned} \tag{17}$$

The solution is straightforward and we see ρ_V evolves like matter with an exponential damping (as expected):

$$\rho_V = \rho_{V0}\left(\frac{R(t)}{R_0}\right)^{-3} e^{-\Gamma t} \tag{18}$$

Now, the effect of this decaying (and the rapidity of thermalisation of V particles) is traduced into an increase of heat per comoving volume, $dQ > 0$, equivalent to the energy added per comoving volume; $-d(R^3\rho_V)$. The latter traduces into:

$$dQ = \Gamma_V \rho_V R^3 dt \tag{19}$$

Now using the thermodynamic definition of entropy (notice that we use here the comoving entropy density), $dS = \frac{dQ}{T}$, we can obtain a diferential equation for the entropy:

$$\dot{S} = \frac{\Gamma_V \rho_V R^3}{T} = a^{1/3} \Gamma_V R^4 \rho_V S^{-1/3} \tag{20}$$

where in the last equality we have used equations (11) and (12) and solved for T. The above equation is a first order equation and can be solved via formal integration:

$$\begin{aligned}
&\int_{S_0}^{S(t)} S^{1/3} dS = \Gamma_V \int_{t_0}^{t} a^{1/3} R^4 \rho_V dt \\
&\xrightarrow[\text{and using (18)}]{\text{Integrating}} \frac{3}{4} S(t)^{4/3} - \frac{3}{4} S_0^{4/3} = \Gamma_V \rho_{V0} R_0^4 \int_{t_0}^{t} a^{1/3} R(t') e^{-\Gamma_V t'} dt' \\
&\implies S(t)^{4/3} = S_0^{4/3} + \frac{4}{3} \rho_{V0} R_0^4 \int_{t_0}^{t} a^{1/3} \left(\frac{R(t')}{R_0} \right) e^{-\Gamma_V t'} d\Gamma_V t'
\end{aligned}$$

Then, using equation (15), $a_0 \equiv a(T = T_0)$ and $S_0^{4/3} = T_0^4 \, R_0^4 \, a_0^{4/3}$ we have $\frac{\rho_{V0} R_0^4}{S_0^{4/3}} = \frac{f_V m_V}{a_0^{1/3} T_0}$ and the above equation takes the form:

$$S^{4/3} = S_0^{4/3} \left[1 + \frac{4}{3} \left(\frac{f_V m_V}{a_0^{1/3} T_0} \right) \int_{t_0}^{t} a^{1/3} \left(\frac{R(t')}{R_0} \right) e^{-\Gamma_V t'} d\Gamma_V t' \right] \tag{21}$$

From this equation we can obtain the dilution factor but we will do some modifications before arriving to the final dilution factor equation. The term that succeeds the unity factor in Eq. (21) tells us what is the effect of the decaying particle in the comoving entropy of the Universe; it contains all the information about V that plays a role in the injection of entropy to the Universe.

At this point, what we ignore is the behaviour of $R(t)$ but we know that the scale factor is governed by the Friedmann's equation and so to solve Eq. (21) we will first need to solve:

$$\left(\frac{\dot{R}}{R} \right)^2 = \frac{8\pi G}{3} \left(\rho_V + \rho_r + \rho_0 \right), \tag{22}$$

where ρ_r is the energy density corresponding to the radiation and ρ_0 is the effective energy density besides relativistic particles in thermal equilibrium and V particles (see paragraph below eq (14) in [14]). However, in the following we will restrict ourselves

to the case, realised in many models, where only ρ_V and ρ_r (i.e. V particles and SM radiation) are taken into account.

To this point, the relevant equations are:

$$\begin{cases} \rho_V &= \rho_{V0}\left(\frac{R(t)}{R_0}\right)^{-3} e^{-\Gamma t} \\ S^{4/3} &= S_0^{4/3}\left[1+\frac{4}{3}\frac{f_V m_V}{a_0^{1/3}T_0}\int_{t_0}^{t} a^{1/3}\left(\frac{R(t')}{R_0}\right)e^{-\Gamma_V t'}d\Gamma_V t'\right] \\ \left(\frac{\dot{R}(t)}{R(t)}\right)^2 &= \frac{8\pi G}{3}\left(\rho_V+\rho_r\right) \end{cases}$$

For the sake of simplification we introduce the adimensional variable $x = \Gamma_V t$ and define the normalised scale factor as

$$z(x) \equiv \frac{R(x)}{R_0}. \tag{23}$$

We also make the following definitions [8]

$$r_V \equiv \frac{\rho_V}{\rho_{V0}}, \qquad r_r \equiv \frac{\rho_r}{\rho_{V0}}, \qquad x_0 \equiv \Gamma_V\sqrt{\frac{3}{8\pi G\rho_{V0}}} = \Gamma_V\sqrt{\frac{3M_{Pl}^2}{\rho_{V0}}} \tag{24}$$

where in the last equation we used $M_{Pl} \equiv 1/\sqrt{8\pi G}$. Then, the system of equations ends up being as follows [9]:

$$\begin{cases} r_V(x) &= \frac{e^{-x}}{z(x)^3} \\ S(x)^{4/3} &= S_0^{4/3}\left[1+\frac{4}{3}\frac{f_V m_V}{a_0^{1/3}T_0}\int_{x_0}^{x} a^{1/3}z(x')e^{-x'}dx'\right] \\ \frac{z(x)'}{z(x)} &= \frac{1}{x_0}\left[(r_V+r_r)\right]^{1/2} \end{cases} \tag{25}$$

Now, the factor between square brackets in second equation of eqs (25) represents the dilution factor (to the 3/4) evaluated at infinity (because we want to compute the dilution factor of the entropy after the decay) and we only have to work on the Friedmann's equation (third one) at this point, to obtain the two equations we want to acquire.

r_r is defined in Eq. (24) and we need the radiation energy density that can be expressed as (from statistical mechanics):

$$\rho_r = \frac{3}{4}aT^4 \tag{26}$$

[8] We can make the last definition because $x_0 = \Gamma_V t_0 \ll 1$ i.e. we can ignore the prefactor (2/3 for a matter dominated Universe or 1/2 for a radiation dominated one) and suppose $t_0 \sim H_0^{-1}$. Also we use $\rho_{V0} \gg \rho_{r0}$ an assumption that will also be used in the numerical integration.

[9] The apostrophe $'$ stands for $\frac{d}{dx}$ and $\frac{d}{dt} = \Gamma_V\frac{d}{dx}$

so, again using eqs (11) and (12) and solving for T, we arrive to:

$$\rho_r = \frac{3}{4}\frac{S^{4/3}}{a^{1/3}\,R^4} \tag{27}$$

At this point it is straightforward to get a useful expression for ρ_r by substituting the second equation of eqs (25)

$$\begin{aligned} \rho_r(x) &= \frac{\rho_{r0}}{z(x)^4} + \frac{S_0^{4/3}}{R_0^4\,a^{1/3}}\frac{f_V m_V}{a_0^{1/3}T_0}\frac{R_0^4}{R(x)^4}\int_{x_0}^{x} a^{1/3}z(x')e^{-x'}dx' \\ \xrightarrow[\text{and } \frac{f_V m_V}{a_0^{1/3}T_0}=\frac{\rho_{V0}R_0^4}{S_0^{4/3}}]{\text{Using (15)}} \rho_r(x) &= \frac{\rho_{r0}}{z(x)^4} + \frac{\rho_{V0}}{a^{1/3}}\frac{1}{z(x)^4}\int_{x_0}^{x} a^{1/3}z(x')e^{-x'}dx' \end{aligned} \tag{28}$$

Then, substituting in the third equation of eqs (25) we finally obtain a general dilution factor expression and the Friedmann's equation for the normalised scale factor:

$$\frac{z(x)'}{z(x)} = \frac{1}{x_0}\left[\frac{e^{-x}}{z(x)^3} + \frac{1}{g_{SM}^{1/3}(x)z(x)^4}\int_{x_0}^{x} g_{SM}^{1/3}(x')z(x')e^{-x'}dx' + \frac{1}{z(x)^4}\frac{\rho_{r0}}{\rho_{V0}}\right]^{1/2} \tag{29}$$

$$D_{SM} = \left(1 + \frac{4}{3}\frac{f_V m_V}{g_{SM}^{1/3}(x_0)T_0}\int_{x_0}^{\infty} g_{SM}^{1/3}(x')z(x')e^{-x'}dx'\right)^{4/3} \tag{30}$$

Here $g_{SM}(x)$ represents the SM degrees of freedom of those particles that are in thermal equilibrium at $x = \Gamma_V t$ (as V particles are not in thermal equilibrium we can write $g_* = g_{SM}$). In the case of a Universe made out of additional particle content such as a Universe with Dark Sector, our computation would be the one corresponding to injection to the SM entropy only and Eq. (30) would be the SM dilution factor (see [12] for more details). That is why we wrote the suffix SM for the dilution factor. Notice, once again, that the dilution factor is the second equation of eqs (25) evaluated at infinity. It can be confusing because it might seem the entropy doesn't depend on x but it does via the upper limit of the integral.

2.2.2 Numerical integration of Friedmann's equation and realising the dilution factor expression

We focus now on the computation of the numerical factor in Eq. (2). At this point is where EMD is realised. The condition is written as $\rho_{V0} \gg \rho_{r0}$ in terms of the energy densities.

With the early matter domination condition the third term inside the squared brackets of Eq. (29) is negligible so we are left with only the two first terms. Now, we can define a new variable we will call $y(x)$ that will help us to absorb the dependence of x_0:

$$y(x) \equiv x_0^{2/3} z(x). \tag{31}$$

Another definition we can make is the one of the averaged d.o.f. during the decay i.e.

$$g_{SM}^{dec} \equiv \left[\frac{\int_{x_0}^{x} g_{SM}^{1/3}(x') z(x') e^{-x'} dx'}{\int_{x_0}^{x} z(x') e^{-x'} dx'} \right]^3 \tag{32}$$

The latter is useful to put outside the integral all the d.o.f. information. Also notice that inside the integral $z(x)e^{-x}$ is maximal when $x = 1$, essentially one can make the approximation $g_{SM}^{dec} \approx g_{SM}(x = 1)$ without producing significant errors in the results (we will use that in the rest of this thesis).

Then, the Friedmann's equation adopts a more workable form:

$$\frac{y(x)'}{y(x)} = \left(\frac{e^{-x}}{y(x)^3} + \frac{g_{SM}^{dec\,1/3}}{y(x)^4 g_{SM}(x)^{1/3}} \int_{x_0}^{x} y(x') e^{-x'} dx' \right)^{1/2} \tag{33}$$

This differential equation can be transformed into a system of first order differential equations by defining another function:

$$P(x) \equiv \int_{x_0}^{x} y(x') e^{-x'} dx'. \tag{34}$$

with its derivative taking the form

$$P(x)' = y(x) e^{-x}$$

The system of first order differential equations one obtains is the following:

$$\begin{cases} y(x)' = \frac{1}{y(x)} \left[y(x) e^{-x} + \frac{1}{g(T_{rad}(\tau_V x))^{1/3}} P(x) \right]^{1/2} \\ P(x)' = y(x) e^{-x} \end{cases} \tag{35}$$

Here g_{SM} depends on the particle's lifetime via the temperature of the thermal bath of a radiation dominated universe $T_{rad}(t = \tau_V x)$ that determines which SM particle is in thermal equilibrium and which is not. Notice that we make the assumption of a radiation dominated universe for our integration. The real temperature of the universe during the EMD and the later particle's decay is different, see section 2.2 of [12]. The dependence on τ_V means we have a different system of equations for each value. We have performed the numerical integration for 1000 values of τ_V and then interpolated the result, still, we haven't observed any deviation from the expressions presented in [16] or [12].

The initial conditions for this system are obtained easily from the definition of $P(x)$, Eq. (34), and from the definition of $z(x)$, Eq. (23), evaluating in $x = x_0$. The initial conditions for $P(x)$ and $y(x)$ are the following:

$$\begin{cases} P(x_0) = 0 \\ y(x_0) = x_0^{2/3} \end{cases} \tag{36}$$

On the other hand, we have to substitute the previous definitions of equations (31) and (32) in the dilution factor equation (30). Using the definition of x_0 in eqs (24) and (15) one arrives to:

$$\begin{aligned} D_{SM} &\overset{(32)}{\simeq} \left(1 + \frac{4}{3}\frac{f_V m_V g_{SM}^{dec\,1/3}}{g_{SM}^{1/3}(x_0)T_0}\int_{x_0}^{x} z(x')e^{-x'}dx'\right)^{4/3} \\ &\overset{(31)}{\Longrightarrow} = \left(1 + \frac{4}{3}\frac{f_V m_V g_{SM}^{dec\,1/3}}{g_{SM}^{1/3}(x_0)T_0}\frac{1}{x_0^{2/3}}\int_{x_0}^{x} y(x')e^{-x'}dx'\right)^{4/3} \\ &\overset{(15)}{\Longrightarrow} = \left(1 + \frac{4}{3}\frac{\rho_{V0} g_{SM}^{dec\,1/3}}{g_{SM}^{4/3}(x_0)T_0^4 x_0^{2/3}}\int_{x_0}^{x} y(x')e^{-x'}dx'\right)^{4/3} \\ \overset{(24)\text{ and }(15)}{\Longrightarrow} D_{SM} &= \left(1 + \left[\frac{4}{3}\left(\frac{2\pi^2}{135}\right)^{\frac{1}{3}}\int_{x_0}^{\infty} y(x)e^{-x}dx\right](g_{SM}^{dec})^{1/3}\left(\frac{m_V f_V}{\sqrt{\Gamma_V M_{Pl}}}\right)^{4/3}\right)^{\frac{3}{4}}. \end{aligned} \tag{37}$$

This is almost eq (2), we need to compute the integral inside the squared brackets and then multiply by the numerical factor in front. The value for that integral corresponds to the value of $P(x)$ at infinity. Infinity can be substituted by $x = 10$ because the integrand is damped by an exponential function and at that point practically all V particles have decayed (i.e. the injection to entropy has finished). Conversely, x_0 can be set as 10^{-3}, as it has to be much smaller than 1 but it cannot be equal to 0.

To obtain the value of $P(x = 10)$, we have integrated numerically via the Python package "*scypi.integrate*" the system of differential equations (35) using the initial conditions in Eq. (36). We have done it in the interval $10^{-3} \lesssim x \lesssim 10$ with a tolerance of 10^{-8}. The code used for this procedure is uploaded in the link provided in appendix A and the result is the following:

Factor inside square brackets of eq (37)
$0.76565048 \pm 0.00000001$

The error comes from the tolerance used to integrate the system of equations (35) and it is only related to the numerical factor in square brackets of equation (37). At the end one can use 0.77 as the numerical factor in the dilution factor expression (37) and find that the real dilution factor's error w.r.t. the complete integration of equation

(30) (i.e. without the assumption that the particle decays after dominating the energy budget of the Universe and the approximation that the SM d.o.f. are constant during the particle's decay) is lower than 10% in the relevant zone for our work at (m_V, τ_V) and $(m_{A'}, \varepsilon)$. As said in the beginning of section 2 this error is computed in appendix A of [12].

2.3 Dilution factor: correlation with particle's free parameters

With equation (2) already justified and having explained its context we can now obtain some results from it. In order to give a general view of the dilution factor's physics w.r.t. the decaying particle's free parameters we have obtained a plot for several values of the dilution factor in the $c\tau_V$ vs m_V plane, see figure 2.

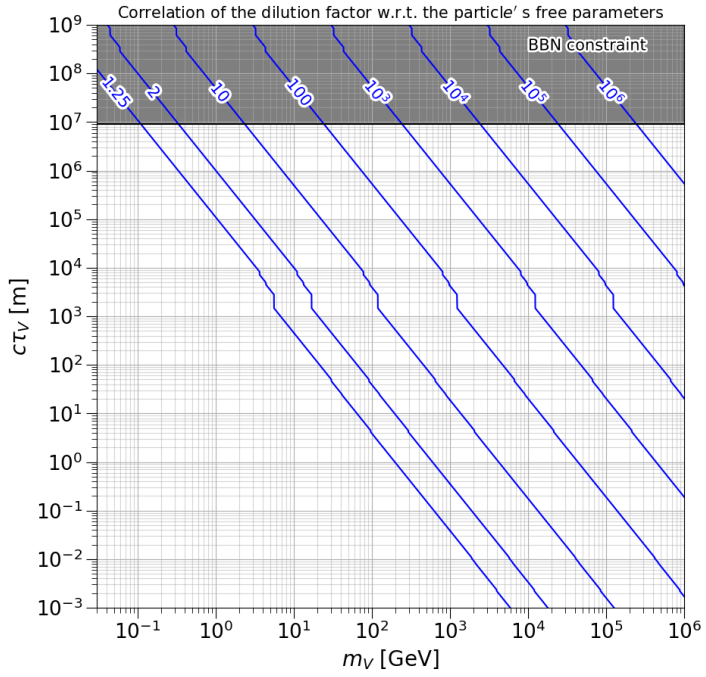

Figure 2: Contour lines of dilution factors in the $(m_V, c\tau_V)$ plane, where m_V is the mass of the decaying particle that injects entropy in the early universe and $c\tau_V$ is its decay length at rest. Grey area represents the zone forbidden by the BBN limit $\tau_V \lesssim 0.03$ as computed in [13].

As one can appreciate there's a feature in all lines for $c\tau_V$ values around $10^3 - 10^4$ meters. This corresponds to the decreasing of the SM degrees of freedom at QCD confinement and other minor decouplings. For the values of $g_{SM}(T)$ we have used table 2

of [21] that encloses the important changes on $g_{SM}(T)$. The plotting has been performed supposing that for $t = \tau_V$ [10] the temperature of the Universe is the same as a Universe without EMD epoch dominated by radiation with age τ_V i.e. $g_{SM}^{dec} \approx g_{SM}(T_{rad}(\tau_V))$ where $T_{rad}(t) = \frac{10^{-3}\text{GeV}\sqrt{2.42\text{s}/t}}{g_{SM}(10^{-3}\text{GeV}\sqrt{2.42\text{s}/t})}$ [11], we reefer to subsection 2.2 of Cirelli et al. [12] for an argued justification. Also we have used 0.02 for the yield f_V which is the value obtained for thermal dark matter and a dark photon that decouples while relativistic (see equation (20) of [20]). We will use the above assumptions and values through the rest of the work.

Notice that for mass values lower than $3 \cdot 10^{-1}$ GeV the dilution factor in the allowed area becomes lower than 2, i.e. the entropy dilutes but its dilution is not significant. To obtain sizeable effects the dilution factor would have to be near 2 or greater, this traduces into a dilutor mass greater than $3 \cdot 10^{-1}$ GeV. Notice that this value is for a freeze-out yield of $f_V = 0.02$ which applies for the dark photon model.

Figure 2 can be useful for experimentalists in search of LLPs at particle colliders. It will give them an idea of the dilution factor zone this new particle could be in. Also it is useful to see that dilution can only be reached if the decaying particle is either a sufficiently long-lived LLP or a very heavy one.

3 Dark Photon and the mixed Higgs sector

In the past decades a great amount of DM candidates and DM mediators, constituting different dark sectors, have been proposed. One of these candidates is the Dark Photon (DP). This particle could represent a DM candidate if produced by the "misalignment mechanism" in the early Universe [22] the same way as axions could have [23] or through the classical thermal production. However, we focus on a heavier range of massive dark photons that decay before BBN, whose role could be the one of mediator between DM and ordinary matter. The DP interacts with SM particles and at the same time with a hypothetical dark sector opening to us a portal to DM also realising in a natural way thermal DM (it could mediate the annihilation process of DM into SM particles, the main process that keeps DM in equilibrium with the thermal bath), see e.g. section 2 of [20].

In the minimal description, the DP is described only by two free parameters, the "kinetic mixing" with the SM photon ε and its mass $m_{A'}$ that can arise from two different mechanisms: Stückelberg mechanism (see Stückelberg articles [24, 25, 26] or [27] for a review) or dark Higgs mechanism (analogous to the Higgs mechanism, we will explain

[10] Because we have to evaluate the SM d.o.f. at $t = \tau_V$, remember that we approximated: $g_{SM}^{dec} \approx g_{SM}(x = 1)$.

[11] In reality what we have is a recurrent function because also the particle's lifetime depends on g_{SM}^{dec} i.e. $g_{SM}^{dec} = g(T_{rad}(c\tau_V(D_{SM}, m_V, g_{SM}^{dec})))$. Substituting recurrently we converge to the real value.

it in section 3.3). The freedom of these two parameters (ε is renormalizable and the mass comes from renormalizable parameters) make the DP model a possible solution for a wide range of problems.

The latter comes with the possibility that the DP could have diluted pre-existing relics. That is because it can fulfill the two main requirements for a particle to dilute relics, listed in the introduction of this thesis. It has the possibility to have a low interaction constant and a low decay width (if it only decays into SM content) making it a LLP (it would be decoupled before it decays) along with the fact that it could have been produced in abundance at early stages of the Universe (thermal production via DM annihilation) fulfilling therefore the first requirement. On the other hand (if sufficiently massive), it could have been non-relativistic when decaying satisfying the second requirement.

In this section we will introduce the DP model when it gets its mass via the dark Higgs mechanism. Then, we will derive (trough the Higgs mixing portal) the DP couling with the SM higgs, $hA'A'$, that will give us the possibility to prove, in the following section, that a long-lived Dark Photon that would have diluted pre-existing relics can be detected by the forthcoming LLP detectors.

3.1 The minimal dark photon model

The dark photon minimal model is a well known extension to the SM of particles where a new massive (or not, but we will not treat this case) vector boson field that transforms under a new $U(1)_{A'}$ symmetry is introduced (first realised by Holdom in the 80's [28, 29]). This carrier of the new abelian force, we will denote by A'_μ, mixes with the SM hypercharge $U(1)_Y$ via the new free adimensional parameter ε refereed to as the "kinetic mixing". This parameter together with the vector boson mass are the two only free parameters added to the theory. Along with the SM lagrangian the spontaneously broken (or Stüeckleberg) $U(1)_{A'}$ lagrangian looks like:

$$\mathcal{L} \supset -\frac{1}{4}\hat{a}_{\mu\nu}\hat{a}^{\mu\nu} - \frac{1}{4}\hat{A'}_{\mu\nu}\hat{A'}^{\mu\nu} + \frac{1}{2}\frac{\varepsilon}{c_W}\hat{A'}_{\mu\nu}\hat{a}^{\mu\nu} + \frac{1}{2}m^2_{A',0}\hat{A'}_{\mu}\hat{A'}^{\mu} \tag{38}$$

where $\hat{a}_{\mu\nu} = \partial_\mu\hat{a}_\nu - \partial_\nu\hat{a}_\mu$ and $\hat{A'}_{\mu\nu} = \partial_\mu\hat{A'}_\nu - \partial_\nu\hat{A'}_\mu$ are the field strength of the hypercharge $U(1)_Y$ and the vector boson $U(1)'_A$ respectively. $m_{A',0}$ is the mass of the DP after $U(1)_{A'}$ symmetry breaking but not yet the mass eigenstate and c_W is the cosinus of the Weinberg angle θ_W.

In order to see clearly the physics of this model one needs to canonically normalise and diagonalise the kinetic terms in Eq. (38). This can be done by the following fields redefinitions:

$$\begin{pmatrix} \hat{A'}_\mu \\ \hat{a}_\mu \end{pmatrix} = \begin{pmatrix} \frac{1}{\sqrt{1-\frac{\varepsilon^2}{c_W^2}}} & 0 \\ \frac{1}{\frac{c_W}{\varepsilon}\sqrt{1-\frac{\varepsilon^2}{c_W^2}}} & 1 \end{pmatrix} \begin{pmatrix} A'_{0,\mu} \\ a_\mu \end{pmatrix} \tag{39}$$

where the "0" subscript of the vector boson A' field redefinition means it is still not the mass eigenstate. If we want to obtain the final mass eigenstate and its corresponding mass eigenvalue we need first to give mass to the massive SM bosons by spontaneously breaking the Electro-Weak symmetry (EWSSB) and then, after applying the above field redefinitions, diagonalise the mass-squared matrix. One can apply the redefinitions in Eq. (39) at any time but has to keep in mind that the hypercharge vector boson which combines with $SU(2)_L$ vector boson b^3_μ after EWSSB is the hatted one present in Eq. (38).

The symmetry breaking traduces into a mixing between the SM $Z_{0,\mu}$ boson (the original SM Z boson after EWSSB) and $A'_{0,\mu}$ (which from Eq. (39) is equivalent to $\hat{A'}_\mu$ except for a multiplying factor) giving rise to the final mass eigenstates. Introducing $\eta = \varepsilon/(c_W\sqrt{1-\frac{\varepsilon^2}{c_W^2}})$ the mass-squared matrix after EWSSB and fields' redefinitions in the massless boson A_μ (carrier of the electromagnetic force), $Z_{0,\mu}$ and $A'_{0,\mu}$ basis $(A_\mu, Z_{0,\mu}, A'_{0,\mu})$ is:

$$\mathcal{M}^2_{NeutralVects} = m^2_{Z,0}\begin{pmatrix} 0 & 0 & 0 \\ 0 & 1 & -\eta s_W \\ 0 & -\eta s_W & \eta^2 s_W^2 + \frac{m^2_{A',0}}{m^2_{Z,0}} \end{pmatrix} \tag{40}$$

Here $m_{Z,0} = v\sqrt{g^2+g'^2}/2 = 91.2$ GeV where $v = 246$ GeV and g (g') is the constant couplig of $SU(2)_L$ ($U(1)_Y$). Notice that the mass-squared matrix is the one of the neutral vector bosons only, that is because only the hypercharge vector boson $\hat{a}_\mu$ mixes with A' and the charged SM bosons $W^\pm_\mu$ aren't composed by it (they are a linear combination of the $SU(2)_L$ vector bosons b^1_μ and b^2_μ). Also, as expected, A_μ remains massless as EM remains unbroken and at the end diagonalising $\mathcal{M}^2_{NeutralVects}$ is equivalent to diagonalise the $(Z_{0,\mu}, A'_{0,\mu})$ sub-matrix. However, although the EM vector boson A_μ seems not to mix in Eq. (40), the truth is that because of the θ_W mixing, α mixing (below) and after canonically normalise (i.e. use Eq. (39)) A_μ actually mixes with A'_μ [12]. The angle of mixing is obtained when $\mathcal{M}^2_{NeutralVects}$ is diagonalised and the relation between the fields before and after the diagonalisation is:

$$\begin{pmatrix} Z_\mu \\ A'_\mu \end{pmatrix} = \begin{pmatrix} \cos\alpha & \sin\alpha \\ -\sin\alpha & \cos\alpha \end{pmatrix} \begin{pmatrix} Z_{0,\mu} \\ A'_{0,\mu} \end{pmatrix} \tag{41}$$

[12] $A_{0,\mu} = s_W\hat{a}_\mu + c_W b^3_\mu$ is the SM photon after EW symmetry breaking. Then, applying Eq. (39) and diagonalising the mass-squared matrix (i.e. using Eq. (41)) yields $A_{0,\mu} = \eta s_W(\sin\alpha Z_\mu + \cos\alpha A'_\mu) + A_\mu$, where we have redefined the EM photon as $A_\mu = s_W a_\mu + c_W b^3_\mu$. This yields the normal EM interactions and new ones proportional to ηs_W.

with an angle of mixing α that follows from the next equation

$$\tan\alpha = \frac{1-\eta^2 s_W^2 - \delta^2 - \text{Sign}(1-\delta^2)\sqrt{4\eta^2 s_W^2 + (1-\eta^2 s_W^2 - \delta^2)^2}}{2\eta s_W} \tag{42}$$

where $\delta = \frac{m_{A',0}}{m_{Z,0}}$ and the convention followed is that for $\varepsilon \to 0$ the angle α goes also to 0. On the other hand, the mass eigenvalues are

$$m^2_{A',Z} = \frac{m_{Z,0}}{2}\left(1+\delta^2+\eta^2 s_W^2 \pm \text{Sign}(1-\delta^2)\sqrt{(1+\delta^2+\eta^2 s_W^2)^2 - 4\delta^2}\right) \tag{43}$$

The mass eigenvalues at order 2 in ε when $\delta \ll 1$ are

$$m^2_Z \approx m^2_{Z,0}(1+\varepsilon^2\tan^2\theta_W), \qquad m^2_{A'} \approx m^2_{A',0}(1-\varepsilon^2\tan^2\theta_W) \tag{44}$$

Notice that for small values of ε the new masses are practically equal to the masses before diagonalising. In our results ε is indeed small and the Z boson and the A' boson mass eigenstates won't depend on ε for small δ. For other values of δ, ε is small compared with δ and we approximate that masses still don't depend on the kinetic mixing, see equation (43) (in the case of $\delta = 1$ we get straightforward from Eq. (43) that $m_Z = m_{A'} = m_{Z,0} = m_{A',0}$).

So we know that the SM Z boson and the SM photon actually mix with A' and how they mix. This gives rise to interactions between SM particles and A'. The dark photon is a particle that can decay into SM particles via the hypercharge portal. In fact, through the (weak) EM interaction between the (Z boson) photon and fermions ($Zf\bar{f}$ and $Af\bar{f}$), one gets a new exchange between the dark photon and SM fermions crucial for its total decay width, see Eq. 45. When calculations are performed the decay width of A' to Z and $W^\pm_\mu$ are negligible w.r.t. the decay widths of A' into fermions. Therefore, as we will need the total decay width, we will only take into account the decays into SM fermions, see subsection 2.2 of [20].

Now, the $A'f\bar{f}$ coupling constant, at LO and after all the procedure explained above, is the following:

$$\begin{aligned} \mathcal{L} &\supset g_{A'f\bar{f}} A'_\mu f\gamma^\mu \bar{f}, \\ g_{A'f\bar{f}} &\equiv \frac{e}{c_W s_W}\left(-\sin\alpha(t^3\ c_W^2 - Y_f s_W^2) + \eta\cos\alpha\ s_W Y_f\right), \end{aligned} \tag{45}$$

where t^3 and Y_f are the fermions' weak isospin and hypercharge values respectively. Of course, e is the usual electromagnetic coupling. A perturbative expansion in ε of the coupling constant gives a good insight of how the DP interacts with SM fermions depending on its mass. From [20] we get the perturbative expansion at LO:

$$g_{A'f\bar{f}} = \varepsilon e\left(Q_f\frac{1}{1-\delta^2} + \frac{Y_f}{c_W^2}\frac{\delta^2}{\delta^2-1}\right) + O(\varepsilon^2) \tag{46}$$

where Q_f is the fermion's electric charge. It is easy to see that when $m_{A',0} \ll m_{Z,0}$ the coupling is photon-like proportional to the fermion's electric charge (this comes from the mixing with the EM vector boson of the SM and is the reason why A' was dubbed as "dark photon"). On the other hand, for values $m_{A',0} \gg m_{Z,0}$ (i.e. when $U(1)_Y$ is not broken) the coupling is proportional to the hypercharge. It should be noted that Eq. (46) is not valid for values of $\delta \sim 1$ and we will use for our computations Eq. (45), valid in all the range of δ. Indeed, the explicit form at LO for $\delta \sim 1$ is "Z-like" i.e.

$$g_{A'f\bar{f}} \overset{\delta\sim 1}{\simeq} \frac{\varepsilon e}{c_W s_W}(t^3\ c_W^2 - Y_f s_W^2) \tag{47}$$

that can be obtained using equations (42) and (45).

The decay width into two fermions can be computed at LO as a decay width of a massive vector boson into two fermions with axial and vectorial couplings:

$$\Gamma(A' \to f\bar{f}) = \frac{N_c}{24\pi} m_{A'} \sqrt{1 - \frac{4m_f^2}{m_{A'}^2}} \left[g_R^2 + g_L^2 - \frac{m_f^2}{m_{A'}^2}(g_R^2 + g_L^2 - 6 g_R g_L) \right] \tag{48}$$

where $g_{R,L} = g_{A' f_{R,L} \bar{f}_{L,R}}$, $Y_{f=l_R,l_L,u_R,u_L,...} = -1, -1/2, 2/3, 1/6, ...$ and $t^3_{f=f_R,\mathrm{u}_L,\mathrm{d}_L} = 0, -1/2, 1/2$[13]. Of course, m_f is the fermion's mass.

3.2 Decay width estimation

The LO expressions are a good approximation only at low and high masses because QCD corrections, hadronic resonances and threshold effects are not negligible for masses in between. Quarks are confined for a center of mass energy ($\sqrt{s} = m_{A'}$) below the $b\bar{b}$ threshold and we have to take that into account. For our computations we used the results for the decay length of figure 2 (right) in [30] when $\varepsilon = 10^{-2}$ and for values $\varepsilon < 10^{-2}$ we extrapolated supposing the decay width is proportional to ε^2 as one can see in Eq. (46). As [30] data does not enclose all the DP mass range we want we used the LO expressions above to compute the DP decay width out of Curtin et al. [30] data range that goes from 0.1 GeV to 65 GeV.

We will briefly explain the procedure in [30] used to obtain the DP decay width and then present our results using LO expressions outside the Curtin et al. [30] mass range. To do that we need to define the ratio

$$R_{A'} = \frac{\Gamma(A' \to \text{hadrons})}{\Gamma(A' \to \mu^-\mu^+)} \overset{\varepsilon\ll 1}{=} R_{A'}(m_{A'}) \tag{49}$$

If we know this ratio we can obtain the total width of the DP multiplying by the LO dark photon to two muons decay width, $\Gamma(A' \to \mu^-\mu^+)$, and summing the rest LO

[13] Here u and d reefers to the upper component and the down one of the $SU(2)_L$ duplet respectively.

expressions (A' decays into leptons). Keep in mind that this procedure is valid for low masses because for higher masses (> 5 GeV, we adopted the same criteria as in section 2.2 of [20]) quarks are no longer confined. Now, for energies < 12 GeV as it is described in [30] the DP coupling is "photon-like" up to corrections order δ^2 and they are corrections that represent less than a 2% of the total coupling. In addition, the experimental ratio

$$R(s) \equiv \frac{\sigma(e^- e^+ \to \text{hadrons})}{\sigma(e^- e^+ \to \mu^- \mu^+)} \tag{50}$$

is highly dominated by off-shell $\gamma^* \to f\bar{f}$ for masses < 12 GeV and it is highly accurate to use experimental data to obtain $R_{A'}(m_{A'}) = R(m^2_{A'})$. For higher energies (where resonances and thresholds start to be less frequent) 3-loop QCD corrections are used in [30] to compute $R_{A'}(m_{A'})$ substituting SM couplings between (axial) vector current and quarks by the couplings of Eq. (45). In figure 3 we present the branching ratios of A' decays into SM fermions where we highlight the confinement zone ($\Lambda_{QCD} = 350$ MeV $< m_{A'} < 5$ GeV) and the range of masses where we used data from [30].

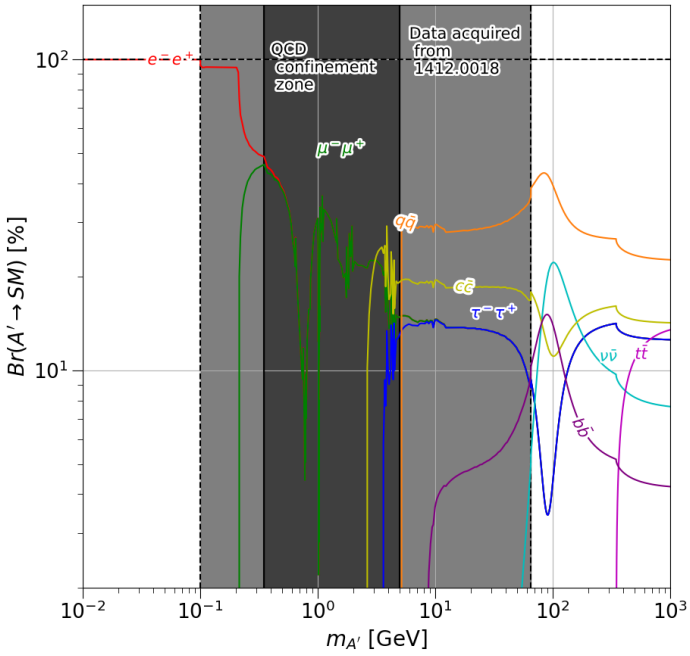

Figure 3: Branching ratios of A' into SM fermions.

One can see clearly a bump at low and high masses joints between our LO computations and [30] data. We estimated the difference and it represents approximately

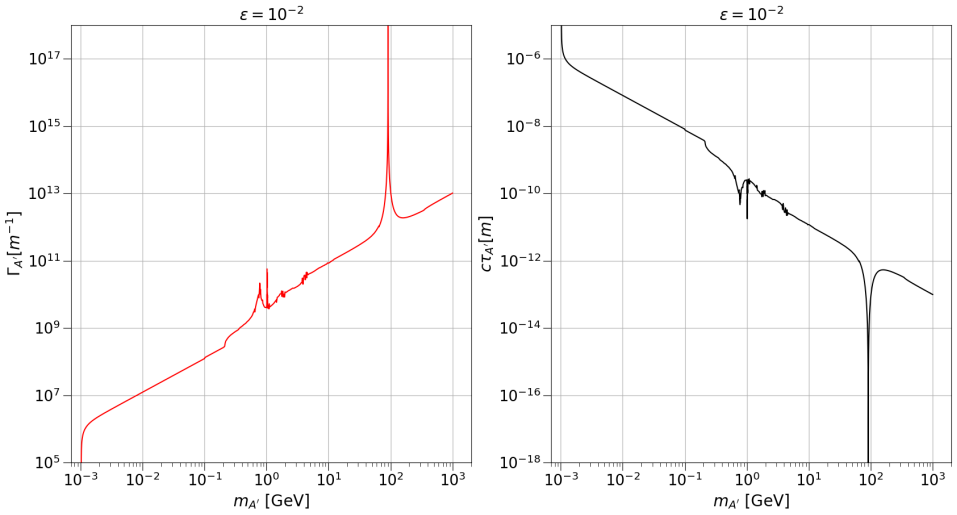

Figure 4: *Left:* Total decay width of the dark photon supposing it only decays into SM fermions. *Right:* Decay length of the dark photon supposing it only decays into SM fermions. Both, the decay width and the decay length, correspond to a value of ε equal to 10^{-2}.

a 6% at low and high masses which is consistent with a bad digitalization of Curtin et al. [30] data (the line width is significantly high enough to yield an error this size). The total decay width is displayed in figure 4 for the dark photon mass interval: 10^{-3} GeV $< m_{A'} < 10^{3}$ GeV. As one can see the bump is hardly appreciated, the same happens with the dilution lines in figure 12. We will use this result for the rest of this thesis. Also, it is remarkable to notice that the decay $h \to A'A'$ is possible in this model but it is highly suppressed by a ε^4 factor as it requires both Z's to mix with A' in the $h \to ZZ^{(*)}$ decay, see [31]. A sizeable $h \to A'A'$ decay is instead produced by the Higgs mixing portal and that will be our focus in the next section.

3.3 Mixed Higgs sector

A massive dark photon can be obtained via two well-known mechanisms: the Stückelberg mechanism and the dark Higgs mechanism. In this section we will explain how the latter mechanism together with the mixing between the SM Higgs and the dark Higgs could give rise to a decay of the SM Higgs into two dark photons. This decay can form part of the invisible Higgs BR and can be measured in the upcoming LLPs detectors providing new information on the dark photon's parameter space $(m_{A'}, \varepsilon)$. That will be our focus in the next section.

The minimal potential describing this theory is the following:

$$V(H,S) = -\mu^2|H|^2 + \lambda|H|^4 - \mu_S^2|S|^2 + \lambda_S|S|^4 + \kappa|S|^2|H|^2 \tag{51}$$

where S is the new dark Higgs singlet with $U(1)_{A'}$ charge q_S, H is the higgs SM $SU(2)_L$ doublet and κ the new mixing parameter between the SM Higgs and the dark Higgs boson. The rest of constants are added as usual to make the terms have the good dimension[14].

The way dark photon obtains its mass through the dark Higgs mechanism is realised easily. The dark Higgs kinetic term takes the form

$$D_\mu S(D^\mu S)^* = (\partial_\mu + ig_{A'}q_S A'_\mu)S(\partial^\mu - ig_{A'}q_S A'^\mu)S^* \tag{52}$$

where $g_{A'}$ is the $U(1)_{A'}$ coupling constant. If the dark Higgs has a non-zero vacuum value i.e. $U(1)_{A'}$ can be broken and $\langle S\rangle = v_S/\sqrt{2}$, infinitesimal fluctuations around it will provide the dark photon a mass equal to

$$\frac{v_S^2}{2} g_{A'}^2 q_S^2 A'_\mu A'^\mu \Rightarrow m_{A',0} = g_{A'}q_S v_S \tag{53}$$

as one can infer from Eq. (52). This is exactly the same mass that appeared in the dark photon minimal model lagrangian (Eq. (38)).

When the SM Higgs also have a non-zero vacuum value i.e. $SU(2)_L$ can also be broken and $\langle H\rangle = \begin{pmatrix} 0 \\ \frac{v}{\sqrt{2}} \end{pmatrix}$ one can express μ and μ_S constants in terms of λ, λ_S, v, v_S and κ

$$\mu^2 = \lambda v^2 + \frac{1}{2}\kappa v_S^2, \qquad\qquad \mu_S^2 = \lambda_S v_S^2 + \frac{1}{2}\kappa v^2 \tag{54}$$

As $\langle S\rangle \neq 0$ and $\langle H\rangle \neq 0$ we can have both symmetries, $U(1)_{A'}$ and $SU(2)_L$, spontaneously broken. In order to have our desired SM Higgs to dark photons decay this needs to happen.

Our objective is to find the mass eigenstates and eigenvalues after the breakings since these are the physical states and values at lab energies. To do that, as the Higgs mechanism demands, we consider small fluctuations h_0 and s_0 around the vacuum minimums of both Higgs fields i.e.

$$H = \begin{pmatrix} 0 \\ \frac{h_0+v}{\sqrt{2}} \end{pmatrix}, \qquad\qquad S = \frac{s_0 + v_S}{\sqrt{2}} \tag{55}$$

[14] μ and μ_S have mass dimension 1, on the other hand λ, λ_S and κ are dimensionless constants.

which substituted in Eq. (51) yields without developing terms

$$V(H,S) = -(\lambda v^2 + \frac{1}{2}\kappa v_S^2)\left(\frac{h_0+v}{\sqrt{2}}\right)^2 + \lambda\left(\frac{h_0+v}{\sqrt{2}}\right)^4 - (\lambda_S v_S^2 + \frac{1}{2}\kappa v^2)\left(\frac{s_0+v}{\sqrt{2}}\right)^2 + \lambda_S\left(\frac{s_0+v}{\sqrt{2}}\right)^4 + \kappa\left(\frac{s_0+v}{\sqrt{2}}\right)^2\left(\frac{h_0+v}{\sqrt{2}}\right)^2 \tag{56}$$

here we have used also equations (54). From the expression above we can obtain the mass terms among which (because of the mixing) there will be non-diagonal terms

$$\begin{aligned} O(h_0^2) + O(s_0^2) + O(h_0 s_0) &= -(\cancel{\lambda v^2} + \frac{1}{2}\cancel{\kappa v_S^2})\frac{h_0^2}{2} + \lambda v^2\cancel{\frac{h_0^2}{2}} + \lambda v^2 h_0^2 \\ &\quad - (\cancel{\lambda_S v_S^2} + \frac{1}{2}\kappa v^2)\frac{s_0^2}{2} + \cancel{\lambda_S v_S^2}\frac{s_0^2}{2} + \lambda_S v_S^2 s_0^2 \\ &\quad + \cancel{\kappa v^2}\frac{s_0^2}{4} + \cancel{\kappa v_S^2}\frac{h_0^2}{4} + \kappa v_S v h_0 s_0 \\ &= \lambda v^2 h_0^2 + \lambda_S v_S^2 s_0^2 + \kappa v_S v h_0 s_0 \\ &= \frac{1}{2}(h_0, s_0)\mathcal{M}^2_{h_0 s_0}\begin{pmatrix} h_0 \\ s_0 \end{pmatrix} \end{aligned}$$

and the squared-matrix $\mathcal{M}^2_{h_0 s_0}$ is therefore

$$\mathcal{M}^2_{h_0 s_0} = \begin{pmatrix} 2\lambda v^2 & \kappa v_S v \\ \kappa v_S v & 2\lambda_S v_S^2 \end{pmatrix} \tag{57}$$

The presence of non-diagonal elements means h_0 and s_0 mix and that, when diagonalising $\mathcal{M}^2_{h_0 s_0}$, the mass eigenstates will be related to h_0 and s_0 via a 2D rotation with an angle θ_h. This is written in matrix language as

$$\begin{pmatrix} h \\ s \end{pmatrix} = \begin{pmatrix} \cos\theta_h & -\sin\theta_h \\ \sin\theta_h & \cos\theta_h \end{pmatrix}\begin{pmatrix} h_0 \\ s_0 \end{pmatrix} \tag{58}$$

The angle satisfies the following equation:

$$\tan\theta_h = \frac{\lambda v^2 - \lambda_S v_S^2 - \text{Sign}(\lambda v^2 - \lambda_S v_S^2)\sqrt{(\lambda v^2 - \lambda_S v_S^2)^2 + \kappa^2 v_S^2 v^2}}{\kappa v_S v} \tag{59}$$

and we will have that the mass eigenstates take the form

$$m^2_{h,s} = v^2\lambda + v_S^2\lambda_S \pm \text{Sign}(\lambda v^2 - \lambda_S v_S^2)\sqrt{(\lambda v^2 - \lambda_S v_S^2)^2 + \kappa^2 v_S^2 v^2} \tag{60}$$

So because of the mixing term in Eq. (51) we see that the SM and dark Higgses in fact mix. This entails new interactions, all particles which interplay with the SM Higgs also interplay with the dark Higgs and vice versa. These new exchanges are controlled by the new parameter θ_h.

Among them there's the interaction between s_0 and A' [15] (which one can obtain from the dark Higgs kinetic term in Eq. (52) after $U(1)_{A'}$ symmetry breaking). This interaction yields a new exchange between the SM Higgs and dark photons because of the H and S mixing ($s_0 = -\sin\theta_h h + \cos\theta_h s$ in the eigenstates' basis) that brings the possibility of a SM Higgs decay into two dark photons. The vertex is (using eqs (52) and (55)):

$$\mathcal{L}_{\cancel{SU(2)_L},\cancel{U(1)_{A'}}} \subset -\frac{m_{A'}^2}{v_S}\sin\theta_h h A'_\mu A'^\mu \tag{61}$$

For a small mixing parameter $\kappa \ll 1$ the exchange will be also proportional to it. Indeed

$$\begin{aligned}\tan\theta_h \approx \sin\theta_h &\approx \frac{\lambda v^2 - \lambda_S v_S^2 - (\lambda v^2 - \lambda_S v_S^2)\left(1 + \frac{\kappa^2 v^2 v_S^2}{(\lambda v^2 - \lambda_S v_S^2)^2}\right)}{\kappa v_S v} \\ &= \frac{\kappa}{2}\frac{v_S v}{\lambda_S v_S^2 - \lambda v^2}\end{aligned} \tag{62}$$

So from Eq. (61) and the approximation above we finally obtain

$$\kappa\frac{1}{2}\left(\frac{m_{A'}^2 v}{\lambda v^2 - \lambda_S v_S^2}\right) h A'_\mu A'^\mu \overset{\kappa\ll 1}{\simeq} \kappa\left(\frac{m_{A'}^2 v}{m_h^2 - m_s^2}\right) h A'_\mu A'^\mu \tag{63}$$

This means the coupling between the SM Higgs and the dark photon is

$$g_{hA'A'} \equiv \kappa\left(\frac{m_{A'}^2 v}{m_h^2 - m_s^2}\right) \tag{64}$$

for small κ. Note that we have used $m_s \approx \lambda_S v_S^2$ and $m_h \approx \lambda v^2$, we can do this for $\kappa \ll 1$ (see equation (60)). We can now compute the LO decay width of the SM Higgs into two dark photons using the well established SM decay of Higgs into two W bosons substituting the SM coupling by Eq. (64) and the W boson mass by the dark photon mass $m_{A'}$ (see equation (2.68) of [32] using that the coupling hW^+W^- is gm_W and $\frac{G_F}{\sqrt{2}} = \frac{g^2}{8m_W^2}$)

$$\Gamma(h \to A'A') = \frac{1}{64\pi}\frac{k'^2 v^2}{m_h}\sqrt{1 - \frac{4m_{A'}^2}{m_h^2}}\left(1 - 4\frac{m_{A'}^2}{m_h^2} + 12\frac{m_{A'}^4}{m_h^4}\right) \tag{65}$$

[15] The vertex is $g_{A'}^2 q_S^2 v_S s_0 A'_\mu A'^\mu$.

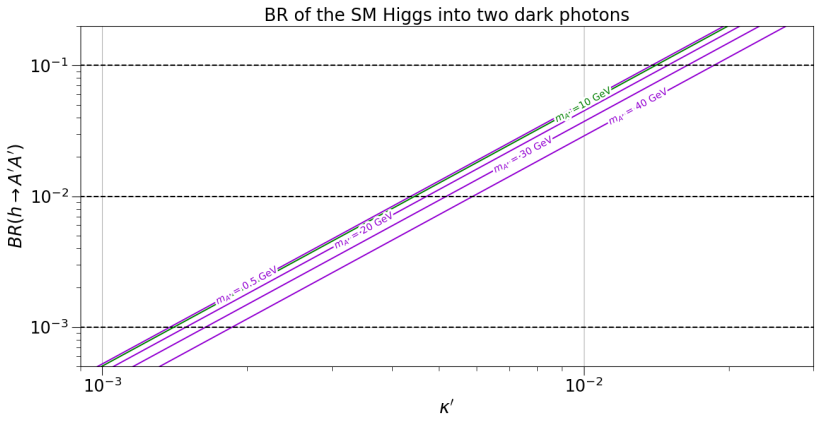

Figure 5: The branching ratio of the SM Higgs decay into two dark photon is represented as a function of κ' defined in Eq. (66). The different lines are computed for dark photon's mass values within the upcoming detectors' range (see subsection 4.2.2 for the particular mass values used for each detector). 10 GeV line is depicted in green to avoid confusions with the 0.5 GeV line. The Horizontal lines are the BR used to represent the detectors' sensitivities in the dark photon parameter space (see results in section 4).

where

$$\kappa' \equiv \frac{\kappa m_h^2}{|m_h^2 - m_s^2|} \tag{66}$$

We have therefore deduced that in the presence of a Higgs mixed sector between a singlet $U(1)_{A'}$ dark Higgs S and the $SU(2)_L$ SM Higgs the decay $h \to A'A'$ is possible and that it is controlled by the mixing parameter. Also the mechanism through which the dark photon gets a mass is necessary to realise it.

Now, the next step is to see if this decay width can yield a measurable contribution (while keeping κ small) to the Higgs total decay width because, as experiments has shown, there's approximately a 10% error in the measured Higgs decay width and therefore room for BSM physics (the invisible Higgs BR actually computed by ATLAS collaboration 10.7 (7.7)% at the 95% CL [33]). In that 10% is where a hypothetical $h \to A'A'$ decay could enter and represent a significant (or a small) contribution. This branching ratio can be measured, if it is not so small, in expected LLP detectors along with the dark photon decay length constraining the dark photon parameter space (see section 4).

To confirm if sizeable BRs with small κ' are possible we have represented the Higgs branching ratio of the dark photon's channel in figure 5. Just looking at the plot we observe that it is indeed viable to produce these BRs via the dark Higgs portal while having a small κ'. We leave in table 1 the κ' values for the different BR's and $m_{A'}$ values used in section 4 i.e. the intersection between the dashed lines and solid ones in figure 5. On the other hand, we have also represented in figure 6 the value of κ vs the dark Higgs

mass m_s. Looking at figure 6 we can see that there are values of the dark Higgs mass from which, if the dark Higgs mass is higher, κ cannot be considered small compared to 1 and eqs (66) and (65) are not valid. We represented this non perturbative zone (defined as $\kappa > 0.25$) in grey. We also show in table 2 the dark Higgs masses for which κ is equal to 0.25 for each value of κ' presented in table 1. In the following section we will take advantage of the fact that a sizeable BR of the SM Higgs decaying into two dark photons can be obtained via the mixed Higgs sector to represent the forthcoming detectors' reach in the dark photon parameter space. However, we have to keep in mind that our analysis is not valid for all dark Higgs masses and to be conservative we will assume that the dark Higgs mass is lower than 475.8 GeV (which is the lowest value in table 2).

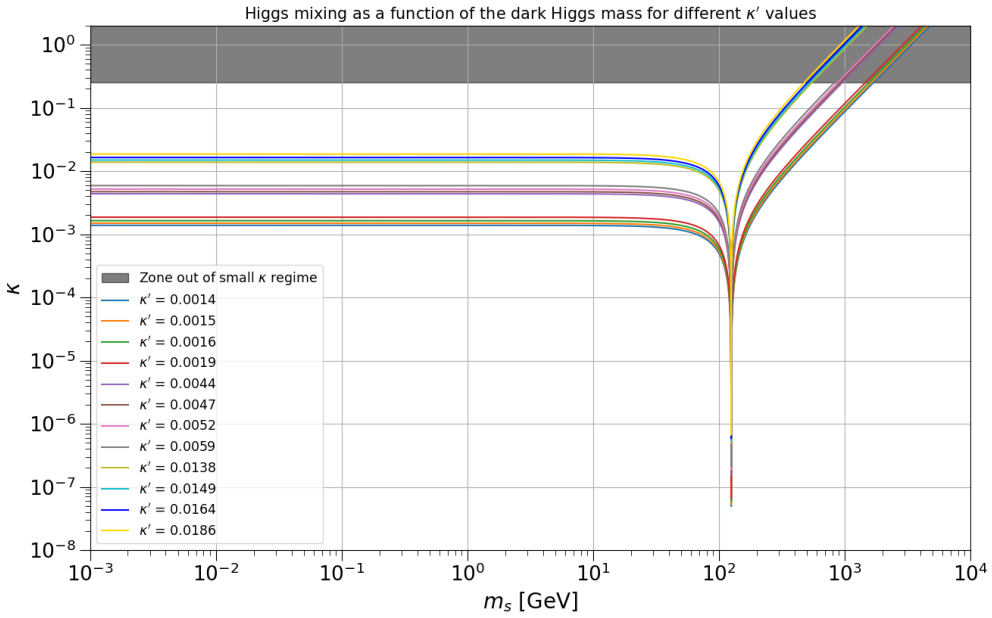

Figure 6: Higgs mixing parameter κ as a function of the dark Higgs mass m_s for the different values of κ' present in table 1. The zone out of the small κ regime is defined by the condition $\kappa > 0.25$ and it is depicted in grey. We computed the mass from which κ is comparable to the unity for every value of κ' and included them in table 2.

	$m_{A'}$ $[GeV]$			
$BR(h \to A'A')$	0.5	10	20	40
0.1	0.014	0.015	0.016	0.019
0.01	0.0044	0.0047	0.0052	0.0059
0.001	0.0014	0.0015	0.0016	0.0019

Table 1: Table of the different values of $\kappa' = \frac{\kappa m_h^2}{|m_h^2 - m_s^2|}$ for the branching ratios used in section 4 and for different values of $m_{A'}$ in the combined range of CODEX-b, ANUBIS and MATHUSLA.

	$m_{A'}$ [GeV]			
$BR(h \to A'A')$	0.5	10	20	40
0.1	547.10	527.73	504.87	475.81
0.01	955.29	920.19	878.70	825.82
0.001	1688.76	1625.94	1551.67	1456.94

Table 2: Table of the different dark Higgs mass values in GeV from which for higher dark Higgs masses the small κ regime ($\kappa \leq 0.25$) does not apply and therefore neither eqs (66) and (65). We obtained them for each one of the κ' values presented in table 1.

4 Diluent dark photon at forthcoming LLP detectors

The objective of this work is to test the sensitivity of three of the upcoming LLP transverse detectors to a diluent DP. Roughly estimating the orders of magnitude of the kinetic mixing and mass of a diluting DP (i.e. a dark photon that dilutes with a factor of 2), the fast conclusion one could arrive is that actual experiments would hardly be sensitive to it. Therefore, one could think that this diluent DP is quite far for being discovered. However, as we have done in this work, by translating into the DP parameter space the sensitivities of CODEX-b, ANUBIS and MATHUSLA, which are based on the exotic Higgs decay into two dark photons, a diluent DP is actually detectable with significant confidence. In this section we will talk about the general LLP detectors' status and report, along with a description of CODEX-b, ANUBIS and MATHUSLA experiments, the procedure carried out to obtain the mentioned results. Then we will show the results and comment them.

4.1 A brief review of the LLP detectors' status

As mentioned before, usually a very low decay rate means negligible particle production at colliders and therefore difficult detection. Nonetheless, technologies and high particle

physics' techniques have been improving in the last decades with a CERN facility very mature at this moment and currently at the 3rd run of its most powerful accelerator: the Large Hadron Collider (LHC). During the last two decades new ideas of LLPs detectors designed to be placed in the LHC or in the Super Proton Synchrotron (SPS) has been proposed and the search of LLPs is on the rise nowadays (see [34] for a review of recent LLP detectors). The most important current, planned or propound LLP experiments during the last few decades can be divided into two types depending on their position w.r.t. the accelerated proton beam (whether the LHC beam or the SPS one):

Forward experiments: These are experiments located in the forward direction of the proton beam that collides with another proton beam (they search within the forward "remnants" of the LHC p-p collision) or with a fixed target (on which SPS protons collide) and can be classified in decay-volume based experiments or proton fixed-target based ones. For example, the most developed forward decay-volume based experiment is FASERν (Forward Search ExpeRiment [35]) located at the LHC tunnel 480 m away from the ATLAS experiment Interacting Point (IP). it is currently working and has already obtained its first results from the LHC run III [36]. On the other hand, proton fixed-target based experiments have already put constraints in the LLP zone of BSM models (such as the DP minimal model, see the νCal constraint in fig 12) and new proposals like the NA62 "beam-dump" mode [37] will test the DP parameter space even further into the LLP zone (see NA62 reach in figure 12). A significantly bigger and general-purpose experiment (again fixed-target based) is planned to be built at the CERN SPS Beam Dump Facility by the name of Search for Hidden Particles (SHiP) [38]. This experiment will be able to dive deeper into the LLP zone of BSM models (see figure 12 for its reach in the DP minimal model case).

Transverse experiments: The transverse experiments are thought to detect particles remnants of beam collisions that are normally produced in the transversal direction[16] and that, because of their long lifetime (LLPs) and weakly interacting character, avoid most LHC experiments' detectors (inner tracker, calorimeters, muon spectrometers....). The transversal direction of these experiments helps to avoid a vast part of the background making them more sensitive than present LLPs searches(one can see this easily in figure 12). One transverse experiment is the imminent COmpact Detector for EXotics at LHCb or CODEX-b (supposed to be partially installed and taking data in 2030 with the LHC run 4 and fully installed in 2035 for the LHC run 5) which has already a prototype CODEX-β that will take data in the current LHC 3rd run and validate background estimates [39]. It is planned to be located at the UX85 experimental cavern of the LHCb a bit ahead of the IP8 and roughly 25m apart from it. Another one is the ANUBIS experiment which has a prototype called proANUBIS already working in ATLAS with very preliminary calibration results obtained in April of this year [40]. The objective is to install ANUBIS last version at the ceiling or in the main shaft (PX14) of

[16]With transversal direction we mean the direction transverse to the proton beam.

ATLAS cavity (see image (a) of figure 9). However, the most ambitious among them is the MAssive Timing Hodoscope for Ultra Stable neutraL pArticles (MATHUSLA) [19], a huge experiment at first thought to have dimensions of 200m×200m×20m (now the design dimensions have changed [41]) centered along the LHC beam line to be built at the surface of the LHC during the HL-LHC programme (currently going on, but not at the time when MATHUSLA was proposed). Due to its ambitious design, and thus elevated budget, it is currently unclear whether MATHUSLA, in that proposed geometry, will ever be realised. However, the MATHUSLA collaboration is working on a revised geometry with reduced size [41]. The functioning and background of each one of these transverse decay-volume based experiments are described in the next section.

We are aware of the existence of other LLP detectors such as SpinQuest [42] or AL3X [43] but we wanted to present a general overview of LLP experiments and explaining all of them goes beyond the focus of this thesis. In figure 7 one can find an sketch of the previous classification w.r.t. the LLP mass, lifetime and the parton center of mass energy.

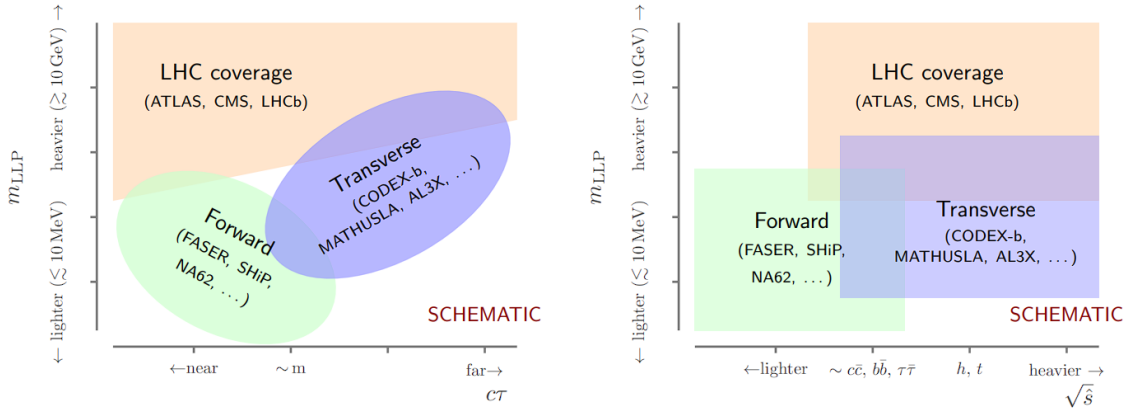

Figure 7: A sketch of the different installed, planed of propound experiments in terms of the LLP mass, lifetime and the parton center of mass energy. **Source:** Aielli et al. [44].

4.2 Testing a diluent dark photon with CODEX-b, ANUBIS and MATHUSLA sensitivities

In this subsection we will describe the three experiments CODEX-b, ANUBIS and MATHUSLA and discuss the associated expected backgrounds to searches for LLPs. Then we will present the procedure followed to cast their sensitivities onto the DP parameter space. In addition, we will also include CMS searches for exotic Higgs decaus into dark photons that later decay into $2d2\bar{d}$ and $2\tau^{+}2\tau^{-}$ presented in [45]. We must mention also analogous searches by ATLAS such as [46] aslo included in our plot (figure 12) or [47] that include constraints on the Higgs boson branching ratio that are the most

stringent to date for $m_s < 40$ GeV and $1 < c\tau_s < 100$ mm (not in the zone we are interested).

4.2.1 CODEX-b, ANUBIS and MATHUSLA description

In order to give some insights of CODEX-b, ANUBIS and MATHUSLA experiments we will describe briefly the design of each of them and introduce their main backgrounds (mainly produced by highly energetic muons produced at the p-p collision):

- **CODEX-b:** the experiment has cubic geometry and consists of six RPC (Resistive Plate Chambers that have cm spacial and ns timing resolution) panels of 10 m^2 conforming the six outer faces of the cube and four additional RPC 10 m^2 panels located in the interior and separated 2 m from each other (one can appreciate this in picture (a) of figure 8). The idea is to measure the signature of the LLP decaying products and reconstruct the LLP mass and decay width (with enough data). To do that one needs to reconstruct the LLP decay vertex and the CODEX-b collaboration has establish 6 as the minimum number of hits per track in order to have a good reconstruction resolution of the decay. Additional minimum track threshold of 600 MeV is also imposed. The backgrounds come principally from SM LLPs such as leptons (μ,...) or neutral hadrons (n, K_L,...). The latter could enter the detector without being detected and decay inside it imitating BSM LLPs. However, the hadrons that come directly from the IP are avoided by a Pb shield that will be placed near the IP8, see picture (a) of figure 8. The location of the experiment allows for an additional passive shield constituted by the UXA concrete wall. Other important source of background are highly energetic muons coming from the IP. When passing through the Pb shield or the concrete shield they could hit atoms and produce hadrons. In order to reject this background a veto is placed inside the Pb shield that will detect muons that trespass it and hit the UXA wall. Hadrons produced in the Pb shield don't pass the UXA concrete wall (image (b) of figure 8) and muons that trespass both shields are vetoed together by the veto station of the Pb shield and the RPC front face.

- **ANUBIS:** this experiment is thought to be installed in the PX14 ATLAS shaft or along the ATLAS cavity ceiling and it will consist in two or more tracking stations (TS) of 100 cm^2 made out of RPC panels that will reconstruct BSM LLP decays. It will be located 80 m from ATLAS and each TS will be positioned 18.5 m apart form each other inside the PX14 ATLAS shaft in its shaft configuration, see figure 9. The authors claim this would be an almost free background experiment following all performance specifications they mention in their proposal [48]. The principal source of background are neutral SM LLP (n, K_L,...) that decay in ANUBIS decay volume. These sources will be vetoed by ATLAS measurements in the calorimeters stations as usually these particles are associated with productions of energetic jet

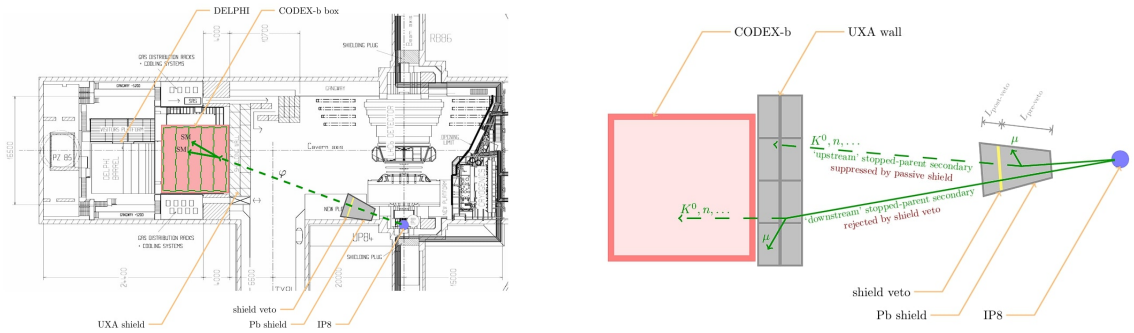

(a) (b)

Figure 8: *(a):* CODEX-b location and structure. *(b):* muon background. **Source:** CODEX-b collaboration[17].

of other hadrons. Other backgrounds are cosmic rays (properly vetoed by the performance specifications listed in [48]), beam-induced backgrounds like beam-gas or beam-collimator collisions (avoided by ANUBIS position) and decays of quasi-thermal neutrons (products lowly energetic and rapidly absorbed). Highly energetic muons are vetoed by the TS. The inconvenient of this experiment is that the PX14 shaft is used during LHC maintenance and in case of an emergency so ANUBIS would have to be designed in order to be easily removed while conserving all its detecting capabilities. The ceiling configuration minimizes the use of ATLAS PX14 shaft (see picture (a) of 9).

- **MATHUSLA:** the experiment (with the revised geometry) has dimensions 100m $\times$100m$\times$25m with 20 m underground. Is thought to be placed 70 m away from the CMS IP in the beam direction. The vertical and horizontal face towards the IP are preceded by scintillator panels, at the surface level it is located a double layer tracker made out of RPCs and at its ceiling a multy layer one, see image (a) of figure 10. The BSM LLP would decay inside MATHUSLA's air filled fiducial volume and its products (for example SM fermions) will leave a signal in the tracking stations. Then, reconstructing the tracks of the decay products, one can reconstruct the decay vertex with the LLP mass and momentum. Regarding the possible backgrounds MATHUSLA, as it is located at the surface, is shielded from most of the ones associated with p-p collisions. However, the location also adds new potential background sources (go to image (b) of figure 10 to see MATHUSLA's backgrounds). Cosmic Rays (CR) muons represent one of the most important backgrounds, nevertheless using timing information at the tracking stations MATHUSLA can discard most of the imitating muon trajectories and a lower frequency is achieved (about 2 Hz for

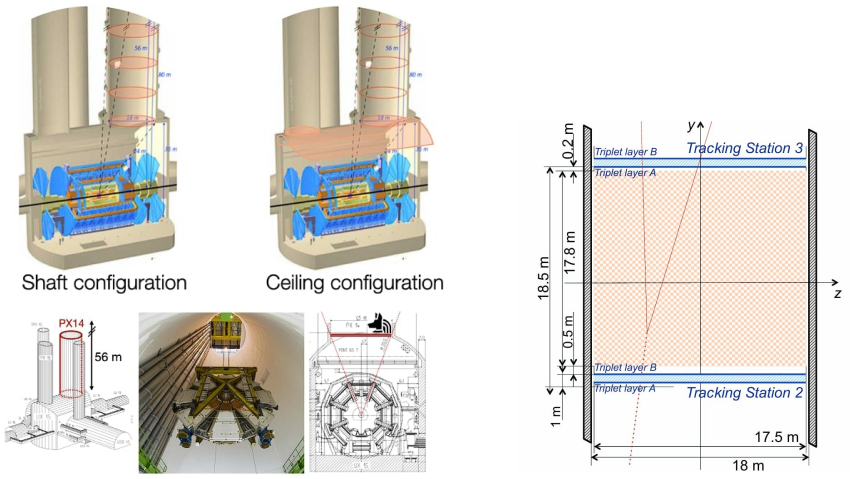

(a) (b)

Figure 9: *(a):* ANUBIS location and possible configurations. *(b):* ANUBIS functioning sketch. It is to say that although the central bottom picture of image (a) seems to be one of ANUBIS tracking stations it is not. These are probably pieces belonging to one of the muon spectometers of ATLAS. **Source:** ANUBIS collaboration [40] and Bauer et al. [48].

a 100 m^2 MATHUSLA)[17]. Other source of background are the muons coming from the LHC that scatter in MATHUSLA's air volume, they will have a frequency of 0.1 Hz for MATHUSLA's actual design. The rest of the background events such as atmospheric neutrinos or muons coming from the LHC that trespass all the space of the experiment can be rejected via the topology of the event or the scintillating veto stations respectively. Neutrinos and muons arriving from LHC that scatter in the air volume background are taken into account at MATHUSLA's proposal paper [19] and after all the cuts the background coming from this cases is 1 per year. As said in the previous section, MATHUSLA's first proposal required a huge budget and the new redimensioned experiment has reduced costs, maybe meaning we will see the beginning of MATHUSLA's construction in the next decades.

[17]Notice that CR travel from up to down in contrast with the LLP decay products and to imitate them they have to do the same trajectory in the opposite direction. This lowers the false events that pass the mentioned timing criteria but muon showers are copiously produced and the CR muon background happens to be of about 2 Hz at the end.

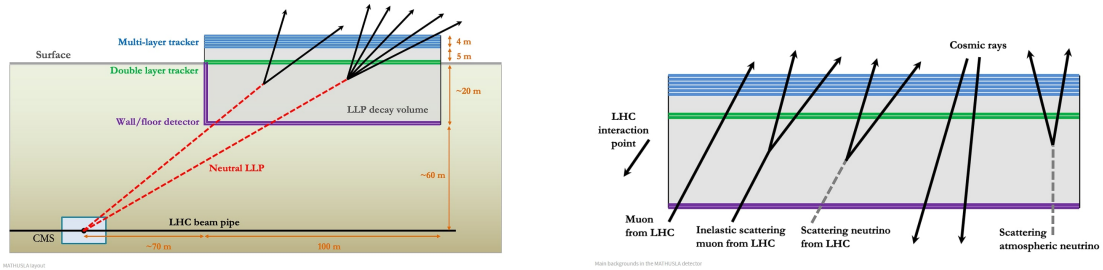

(a) (b)

Figure 10: *(a):* MATHUSLA experiment display. *(b):* MATHUSLA's most important backgrounds. **Source:** MATHUSLA collaboration [41].

4.2.2 Casting the experiments' sensitivities to the minimal dark photon parameter space

The main feature concerning all these three detectors is that they are sensitive to exotic Higgs decays whether into two scalars or into two abelian vector bosons. It is estimated that during the HL-LHC run a total of $1.5 \cdot 10^8$ Higgs will be produced (section II in [19]), so search for invisible Higgs decays is a reasonable idea. As we have proved in the preceding section the Higgs decay into two dark photons for a small Higgs mixing is possible. So we are able to 'translate' the detectors' sensitivity into the DP parameter space.

First of all, we have to notice that sensitivities are given, by the experimental collaborations, as a function of the BR of the exotic Higgs decay into two BSM LLPs $BR(h \to A'A')$ w.r.t. the decay length at rest of the LLPs them selves. Also, each sensitivity line corresponds to a different LLP mass value. Notice as well that sensitivities of decay-volume experiments to exotic Higgs decays present the same hyperbolic-like form, i.e. tending to a line with positive slope for high decay lengths and more or less vertical tendency for low decay lengths (of course, for decreasing BR values the sensitivity decreases also because there are less chances to detect the particle). This form is due to the solid angle that the detector is able to cover times the distance it encloses (divided by a boost factor that depends on the particle's momentum) i.e. it depends on the fiducial decay volume, which at high decay lengths translates into a diagonal limit (the more solid angle and distance are covered the greater is the detectors' sensitivity to longer-lived LLPs). At low decay lengths the possible particle's decay outside the fiducial volume represents a vertical limit.

Keeping all the above in mind, the strategy we followed was to obtain for three BR values, $BR(h \to A'A') = 0.001, 0.01, 0.1$ the detector's sensitivity decay length lower limit and the decay length upper limit (see figure 11) and linearly interpolate points between the different available LLP mass values for which the sensitivity has been computed (the set of masses are determined by each experiment because of the independent

analysis each collaboration have carried out with his detector). The interpolation is performed for the lower limit values and upper limit ones independently. Then, to traduce the data into the $(m_{A'}, \varepsilon)$ parameter space, we have used the decay length data in figure 4 supposing the decay width $\Gamma_{A'}$ is proportional to ε^2 (which it is for the small values of ε we are considering, see eqs 46 and 47) to obtain the points in the $(m_{A'}, \varepsilon)$ plane. The latter procedure yields a band for each BR value as one can see in figure 12.

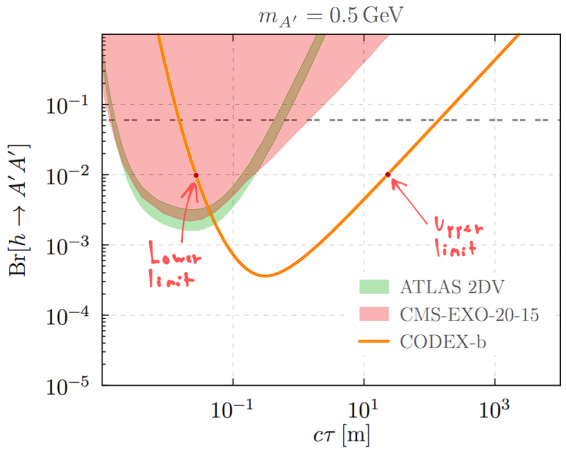

Figure 11: A sketch of the data acquisition for LLP detectors' sensitivity. In the figure it is shown the sensitivity of CODEX-b for a LLP mass of 0.5 GeV and the points extracted correspond to an exotic Higgs BR of 0.01. **Source of the original plot:** Aielli et al. [17]

As we mentioned before, the values of the masses considered are different depending on the experiment. For CODEX-b the collaboration just presents 2 plots for LLP masses values of 0.5 GeV and 10 GeV, one can find the plots in figure 3 of [17]. For the ANUBIS case we have used the line corresponding to 50 events in the ANUBIS ceiling configuration of figure 4.7 in [18] for m_{LLP} =10, 20, 30, 40 GeV. On the other hand, in the MATHUSLA case we have used the data in figure 3 of [19] corresponding to m_{LLP} =5, 20, 40 GeV. Although experiments are indeed sensitive to a larger range of LLP mass values we have been conservative and we have only interpolated between the masses collaborations have published. For our purpose that is enough even though the complete sensitivity of experiments would enclose a greater area in figure 12. The centre of mass energy and the integrated luminosity in these three experiments correspond to the HL-LHC ones, i.e. $\sqrt{s} = 14$ TeV and $\mathcal{L} = 3\ ab^{-1}$.

In addition, we have used this same procedure to include in our plot the 2021 CMS exclusion for a LLP decaying into down quarks and tau leptons. In this case the CMS collaboration presented exclusions corresponding to 4 LLP masses from 7 GeV to 55 GeV included. As one can see in figure 3 of [45] the exclusions are approximately linear w.r.t. the masses so we have just used the 7 GeV and 55 GeV sensitivities and then performed

the linear interpolation mentioned above. The result is presented in figure 12.

4.2.3 Constraints, the dilution zone, experiments' reaches and results in the minimal dark photon parameter space

All the above has finally enable us to recast in the same plot (figure 12): several dilution lines, dark photon exclusions (CMS 2021 exclusion [45]) and upcoming experiments' reach (CODEX-b, ANUBIS and MATHUSLA the most important ones). We have represented the minimal dark photon parameter space for values of the kinetic mixing from 10^{-6} to 10^{-14} and masses between 10^{-3} to 10^{3} GeV.

A diluent dark photon needs to have a low coupling with SM particles i.e. $\varepsilon \ll 1$ (because it is the only free parameter in the coupling, Eq. (46) or Eq. (47)) in order to live long enough to realise an EMD before decaying and high mass to be non-relativistic when that happens. That is why dilution factor lines gather at the bottom right part of our plot 12. We call that zone, defined by $D_{SM} \geq 2$, the dilution zone. The dilution factor lines are obtained equating the decay width of the DP (the one in figure 4) with the decay width required to obtain the desired dilution factor value (solve eq (2) for Γ_V). Supposing the decay width is proportional to ε^2 one can solve for ε acquiring the needed ε for dilution. The latter will depend only on the DP mass (g_{SM}^{dec} depends on the particle's lifetime but the latter also depends on the dilution factor and the particle's mass [18]).

An important constraint on the dark photon minimal model (and almost all BSM models) is the BBN limit. This accounts for the fact that for lifetimes greater or equal to the time of BBN new particle existence in significant amounts (matter domination) would be in contradiction with observations. The baryonic abundances after BBN in our Universe are in excellent concordance with SM alone predictions that foretell radiation domination for that epoch. To represent this limit in the dark photon parameter space we forbid the zone where the dark photon decay length is greater than 0.03 s (limit computed in [13]) and permit the zone where the DP produces a dilution factor lower or equal than 1.1 because in that case the dark photon would not dominate the energy density of the Universe (no dilution or low dilution means no matter domination). Notice that, as said in section 2.3, because of the BBN limit, sizeable dilution ($D_{SM} \geq 2$) is achieved for masses greater or equal than $3 \cdot 10^{-3}$ GeV. Also, the steps in the dilution factor lines are produced by the change of the SM degrees of freedom as in figure 2. The required ε to have dilution is proportional to ${g_{SM}^{dec}}^{1/4}$ and therefore when the SM degrees of freedom decrease the dilution lines in our plot also do so.

[18] To be technically precise what we have is a recurrent function, see footnote 11

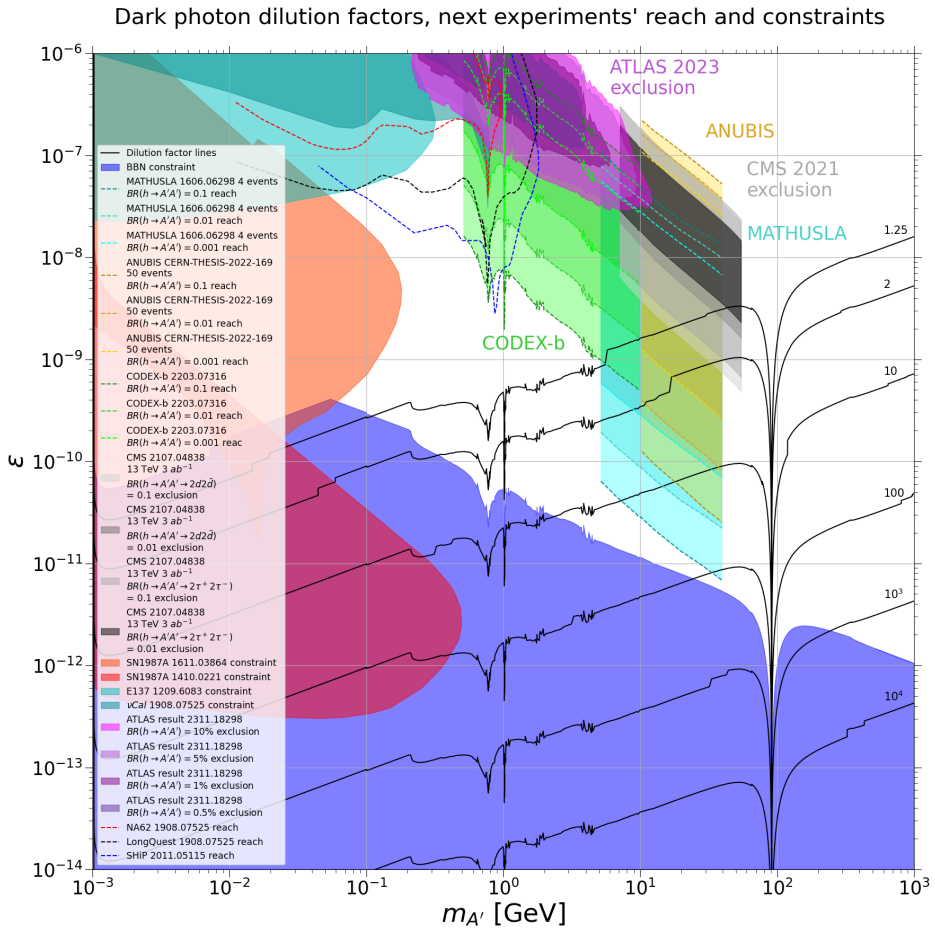

Figure 12: Dark photon parameter space of kinetic mixing ϵ versus mass $m_{A'}$. Black contour lines indicated values form 1.25 to 10^4 of the SM dilution factor D_{SM} as computed in this thesis, where we conventionally define the dilution zone by $D_{SM} \geq 2$. We also display our recast of exclusions and sensitivities to Higgs decays into long-lived dark photons, at CODEX-b [17], ANUBIS [18] and MATHUSLA [19], derived as explained in the main text and for different values of the Higgs BR into dark photons. The CMS exclusion [45] recasted as explained in the main text is also included along with recent ATLAS exclusion [46]. Several other pre-existing constraints are shown: SN1987 constraints of [49] and its later revision [50], νCal updated constraint [51] and the E137 one [52]. There is an additional constraint zone we haven't included and it corresponds to the blob appearing in figure 3 (b) of [51] for $\varepsilon \in (2.5 \cdot 10^{-8}, 8 \cdot 10^{-8})$. We have also added sensitivities for fixed-target based experiments, NA62 [51], SHiP [53] and LongQuest, a retool of the SeaQuest experiment at the Fermilab [51]. The BBN constraint $\tau_{A'} \lesssim 0.03$ sec [13] is also shaded in blue on the bottom-right side of the figure.

All constraints, other than those recasted in this thesis, lie outside the dilution zone (except for the BBN constraint, of course) and the same happens for the fixed-target based experiments' reach. We see a different tendency for the LHC exclusions (ATLAS and CMS ones). They reach higher masses and in the case of the CMS exclusion limits they actually hit the dilution zone. CODEX-b recasted sensitivity also reaches higher masses but it does not touches the dilution zone. However, new frontiers could be opened by ANUBIS and MATHUSLA experiments (as far as dilution by a DP is concerned). We see clearly that both sensitivities dive deeper into the dilution zone and they do it even for an exotic Higgs decay into two dark photons equal to 0.001. This shows the incredible potential of these transverse experiments.

One key aspect in CODEX-b, ANUBIS and MATHUSLA sensitivities and ATLAS and CMS exclusions is that the lower the branching ratio the less is the experiment sensitive to lower values of the kinetic mixing. As said, in our case, the sensitivity depends on the fraction of the Higgs decay width the decay $h \to A'A'$ represents. The objective when we build more sensitive experiments is to detect weaker interactions i.e. lower BRs. Indeed, we have that CMS is not sensitive to a BR of 0.1% (see figure 3 in [45]) and if $BR(h \to A'A') = 0.1\%$ CMS would not be able to exclude the DP parameter space. In addition the CMS exclusions are for dark photon decays into $d\bar{d}$ and $\tau^+\tau^-$ (the decay into d quarks yields more sensitive results) and a dark photon with these decays forbidden independently of the dark photon mass would avoid this exclusion, nevertheless we are not aware of models where that type of dark photon is possible. The forthcoming transverse detectors are much more sensitive and they go from BR around 10^{-4} for CODEX-b to BR around 10^{-5} for ANUBIS and MATHUSLA. We have to keep in mind that the lower the BR the narrower is the zone of reach in the parameter space, we can see that in the sensitivity plots e.g. figure 11. For example, although ANUBIS and MATHUSLA reach BR $= 10^{-5}$ the recast for that BR would be almost a line in the DP parameter space. However, for larger BR, say 10^{-2}, the recast for ANUBIS and MATHUSLA is way wider than the CMS one. The latter is due to the fact that the sensitivity in the $BR(h \to$ BSM particles) vs decay length plane presents a hyperbolic-like form independently of the experiment as we explained in the previous section.

5 Conclusions

Searches for BSM physics have been the thrust of the scientific world (as far as high energy physics is concerned) during the last 50 years. Although some great achievements have been accomplished, we know we are far from understanding the Universe in its whole (so many missing pieces: Dark Matter, Dark Energy, baryon asymmetry, neutrino oscillations, hierarchy problem, strong CP problem,...). However, as human beings we do not cease in our study of the Universe and old and new experiments are redefining

themselves in search for the truth. ATLAS [46, 47] and CMS [45] LLP searches are a good example of existing experiments that, using their available data, find new ways to look for BSM physics, strengthening their potential to discover it. CODEX-b, ANUBIS and MATHUSLA are examples of upcoming or proposed experiments that, focusing on the search of new physics, have adapted their designs to satisfy this task exigencies. Indeed, these experiments' sensitivities outperform the ones of ATLAS and CMS for the search of LLP as one can see just comparing CMS figure 3 on [45] with CODEX-b figure 3 top of [17], the less sensitive of the three upcoming experiments.

Our incomprehension of the Universe shouldn't deprive our motivations. Indeed, new matter content, as needed to solve some of the problems of the SM, also opens the door for new phenomena and new ways to satisfy our curiosity. That is the case of EMD. Although it could only have happened no later than about 0.03 seconds after the Big Bang, the existence of EMD can affect very significantly the manifestations of BSM in the early Universe, ranging from DM to primordial GWs and any other pre-exising relic.

In this thesis we add proofs that motivate the search for LLPs at colliders, in particular for long-lived dark photons that would have dominated the energy budget of the Universe at its early stages. At the beginning we have presented the general correlation between the dilution factor and the LLP's decay width Γ_V and mass m_V, using equation (2). Then we have motivated the Higgs decay into dark photos via the Higgs portal (a natural portal because it explains dynamically the dark photon's mass) where sizeable BRs are achievable (although the analysis for a dark Higgs mass higher than 475.8 GeV is out of the range of this thesis). Finally, we have shown the capacity of new transverse LLP search experiments, CODEX-b, ANUBIS and MATHUSLA to be precise, to explore the dark photon parameter space opening the possibility to detect a diluting dark photon at the LHC. This constitutes a new result of this thesis, because the only paper showing that an EMD could be tested at colliders [16] used glueballs as an example of LLPs, whose early-Universe phenomenology is very different from the one of the dark photons studied here.

The advent of all these BSM searches, developments and the current running of HL-LHC anticipates promising results for the next decade. With this work we have proven that EMD can be actually tested in colliders right now, even for the simplest models.

A GitHub repository

This work has been implemented using Jupyter Notebook, a python web-based interactive computing platform. Below we include a link directly to the GitHub repository containing all .ipynb files and data necessary to reproduce the results.

https://github.com/CarlosGarciaSanchez19/MasterThesisUNIBOTheorPhys

References

[1] Scott Dodelson. *Modern Cosmology*. 1st ed. Academic Press, Mar. 2003. ISBN: 9780122191411.

[2] Marco Cirelli, Alessandro Strumia, and Jure Zupan. "Dark Matter". In: (June 2024). URL: https://arxiv.org/abs/2406.01705v1.

[3] Vera C. Rubin et al. "Rotation of the Andromeda Nebula from a Spectroscopic Survey of Emission Regions". In: *ApJ* 159 (Feb. 1970), p. 379. ISSN: 0004-637X. DOI: 10.1086/150317. URL: https://ui.adsabs.harvard.edu/abs/1970ApJ...159..379R/abstract.

[4] F. Zwicky. "On the Masses of Nebulae and of Clusters of Nebulae". In: *ApJ* 86 (Oct. 1937), p. 217. ISSN: 0004-637X. DOI: 10.1086/143864. URL: https://ui.adsabs.harvard.edu/abs/1937ApJ....86..217Z/abstract.

[5] Douglas Clowe et al. "A direct empirical proof of the existence of dark matter". In: *The Astrophysical Journal* 648 (2 Aug. 2006), pp. L109–L113. DOI: 10.1086/508162. URL: http://arxiv.org/abs/astro-ph/0608407%20http://dx.doi.org/10.1086/508162.

[6] Gianfranco Bertone and Dan Hooper. "A History of Dark Matter". In: *Reviews of Modern Physics* 90 (4 May 2016). DOI: 10.1103/RevModPhys.90.045002. URL: http://arxiv.org/abs/1605.04909.

[7] Gerard Jungman, Marc Kamionkowski, and Kim Griest. "Supersymmetric dark matter". In: *Physics Reports* 267 (5-6 Mar. 1996), pp. 195–373. ISSN: 0370-1573. DOI: 10.1016/0370-1573(95)00058-5.

[8] Jonathan L. Feng. "Naturalness and the Status of Supersymmetry". In: *Annual Review of Nuclear and Particle Science* 63 (Feb. 2013), pp. 351–382. DOI: 10.1146/annurev-nucl-102010-130447. URL: http://arxiv.org/abs/1302.6587%20http://dx.doi.org/10.1146/annurev-nucl-102010-130447.

[9] CERN collaboration. *The Future Circular Collider — CERN*. URL: https://home.cern/science/accelerators/future-circular-collider.

[10] Kim Griest and Marc Kamionkowski. "Unitarity limits on the mass and radius of dark-matter particles". In: *Physical Review Letters* 64 (6 Feb. 1990), p. 615. ISSN: 00319007. DOI: 10.1103/PhysRevLett.64.615. URL: https://journals.aps.org/prl/abstract/10.1103/PhysRevLett.64.615.

[11] Salvatore Bottaro and Diego Redigolo. "The dark matter unitarity bound at NLO". In: (May 2023). URL: https://arxiv.org/abs/2305.01680v1.

[12] Marco Cirelli et al. "Homeopathic Dark Matter, or how diluted heavy substances produce high energy cosmic rays". In: *Journal of Cosmology and Astroparticle Physics* 2019 (2 Nov. 2018). DOI: 10.1088/1475-7516/2019/02/014. URL: http://arxiv.org/abs/1811.03608.

[13] Karsten Jedamzik. "Big bang nucleosynthesis constraints on hadronically and electromagnetically decaying relic neutral particles". In: *Physical Review D - Particles, Fields, Gravitation and Cosmology* 74 (10 Nov. 2006), p. 103509. ISSN: 15507998. DOI: 10.1103/PHYSREVD.74.103509/FIGURES/11/MEDIUM. URL: https://journals.aps.org/prd/abstract/10.1103/PhysRevD.74.103509.

[14] Robert J. Scherrer and Michael S. Turner. "Decaying particles do not "heat up" the Universe". In: *Physical Review D* 31 (4 Feb. 1985), p. 681. ISSN: 05562821. DOI: 10.1103/PhysRevD.31.681. URL: https://journals.aps.org/prd/abstract/10.1103/PhysRevD.31.681.

[15] Yann Guttenoire. "Beyond the Standard Model Cocktail". In: (July 2022). URL: https://arxiv.org/abs/2207.01633v1.

[16] Fady Bishara, Filippo Sala, and Kai Schmidt-Hoberg. "Early Matter Domination at Colliders: Long Live the Glueball!" In: (Jan. 2024). URL: https://arxiv.org/abs/2401.12278v1.

[17] Giulio Aielli et al. "The Road Ahead for CODEX-b". In: (Mar. 2022). URL: https://arxiv.org/abs/2203.07316v1.

[18] Thomas Peabody Satterthwaite. *Sensitivity of the ANUBIS and ATLAS Detectors to Neutral Long-Lived Particles Produced in pp Collisions at the Large Hadron Collider*. 2022. URL: https://cds.cern.ch/record/2839063.

[19] John Paul Chou, David Curtin, and H. J. Lubatti. "New Detectors to Explore the Lifetime Frontier". In: *Physics Letters, Section B: Nuclear, Elementary Particle and High-Energy Physics* 767 (June 2016), pp. 29–36. DOI: 10.1016/j.physletb.2017.01.043. URL: http://arxiv.org/abs/1606.06298.

[20] Marco Cirelli et al. "Dark Matter's secret liaisons: phenomenology of a dark U(1) sector with bound states". In: *Journal of Cosmology and Astroparticle Physics* 2017 (5 Dec. 2016). DOI: 10.1088/1475-7516/2017/05/036. URL: http://arxiv.org/abs/1612.07295.

[21] Lars Husdal. "On Effective Degrees of Freedom in the Early Universe". In: *Galaxies* 4 (4 Sept. 2016). DOI: 10.3390/galaxies4040078. URL: http://arxiv.org/abs/1609.04979.

[22] Kunio Kaneta et al. "Misalignment mechanism for a mass-varying vector boson". In: (June 2023). URL: https://arxiv.org/abs/2306.01291v2.

[23] John Preskill, Mark B. Wise, and Frank Wilczek. "Cosmology of the invisible axion". In: *Physics Letters B* 120 (1-3 Jan. 1983), pp. 127–132. ISSN: 0370-2693. DOI: 10.1016/0370-2693(83)90637-8.

[24] E.C.G. Stueckelberg. "The interaction forces in electrodynamics and in the field theory of nuclear forces (I)". In: *Helv.Phys.Acta* 11 (1938), pp. 225–244. DOI: 10.5169/SEALS-110852.

[25] E.C.G. Stueckelberg. "The interaction forces in electrodynamics and in the field theory of nuclear forces (II)". In: *Helv.Phys.Acta* 11 (1938), pp. 299–312. DOI: 10.5169/SEALS-110852.

[26] E.C.G. Stueckelberg. "The interaction forces in electrodynamics and in the field theory of nuclear forces (III)". In: *Helv.Phys.Acta* 11 (1938), pp. 312–328. DOI: 10.5169/SEALS-110852.

[27] Henri Ruegg and Marti Ruiz-Altaba. "The Stueckelberg Field". In: *International Journal of Modern Physics A* 19 (20 Apr. 2003), pp. 3265–3347. DOI: 10.1142/S0217751X04019755. URL: http://arxiv.org/abs/hep-th/0304245%20http://dx.doi.org/10.1142/S0217751X04019755.

[28] Bob Holdom. "Two U(1)'s and ϵ charge shifts". In: *Physics Letters B* 166 (2 Jan. 1986), pp. 196–198. ISSN: 0370-2693. DOI: 10.1016/0370-2693(86)91377-8.

[29] Bob Holdom. "Oblique electroweak corrections and an extra gauge boson". In: *Physics Letters B* 259 (3 Apr. 1991), pp. 329–334. ISSN: 0370-2693. DOI: 10.1016/0370-2693(91)90836-F.

[30] David Curtin et al. "Illuminating Dark Photons with High-Energy Colliders". In: *Journal of High Energy Physics* 2015 (2 Nov. 2014), pp. 1–45. DOI: 10.1007/JHEP02(2015)157. URL: http://arxiv.org/abs/1412.0018.

[31] David Curtin et al. "Exotic Decays of the 125 GeV Higgs Boson". In: *Physical Review D - Particles, Fields, Gravitation and Cosmology* 90 (7 Dec. 2013). DOI: 10.1103/PhysRevD.90.075004. URL: http://arxiv.org/abs/1312.4992.

[32] R. N. Cahn. "The Higgs boson". In: *Reports on Progress in Physics* 52 (4 Apr. 1989), p. 389. ISSN: 0034-4885. DOI: 10.1088/0034-4885/52/4/001. URL: https://iopscience.iop.org/article/10.1088/0034-4885/52/4/001.

[33] ATLAS Collaboration. "Combination of searches for invisible decays of the Higgs boson using 139 fb^{-1} of proton-proton collision data at $\sqrt{s} = 13$ TeV collected with the ATLAS experiment". In: *Physics Letters, Section B: Nuclear, Elementary Particle and High-Energy Physics* 842 (Jan. 2023). DOI: 10.1016/j.physletb.2023.137963. URL: http://arxiv.org/abs/2301.10731.

[34] Vasiliki A. Mitsou. "LHC experiments for long-lived particles of the dark sector". In: (Nov. 2021), pp. 2029–2049. DOI: 10.1142/9789811269776_0160. URL: http://arxiv.org/abs/2111.03036%20http://dx.doi.org/10.1142/9789811269776_0160.

[35] FASER Collaboration et al. "The FASER Detector". In: (July 2022). URL: https://arxiv.org/abs/2207.11427v1.

[36] FASER Collaboration et al. "First Direct Observation of Collider Neutrinos with FASER at the LHC". In: *Physical Review Letters* 131 (3 Mar. 2023), p. 031801. ISSN: 10797114. DOI: 10.1103/PHYSREVLETT.131.031801/FIGURES/7/MEDIUM. URL: http://arxiv.org/abs/2303.14185.

[37] Babette Döbrich, Joerg Jaeckel, and Tommaso Spadaro. "Light in the beam dump – ALP production from decay photons in proton beam-dumps". In: *Journal of High Energy Physics* 2020 (10 Apr. 2019). DOI: 10.1007/JHEP10(2020)046. URL: http://arxiv.org/abs/1904.02091.

[38] C. Ahdida et al. "The SHiP experiment at the proposed CERN SPS Beam Dump Facility". In: *European Physical Journal C* 82 (5 Dec. 2021). ISSN: 14346052. DOI: 10.1140/epjc/s10052-022-10346-5. URL: https://arxiv.org/abs/2112.01487v2.

[39] Louis Henry. *Update on the CODEX-b Experiment - CERN Document Server (minute 6:08)*. URL: https://cds.cern.ch/record/2897511.

[40] *WebHome ¡ ANUBIS ¡ TWiki*. URL: https://twiki.cern.ch/twiki/bin/view/ANUBIS/.

[41] MATHUSLA collaboration. *Home — mathusla.web.cern.ch*. URL: https://mathusla-experiment.web.cern.ch/.

[42] *SpinQuest — Website for the SpinQuest/E1039 Experiment at Fermilab*. URL: https://spinquest.fnal.gov/.

[43] Vladimir V. Gligorov et al. "Leveraging the ALICE/L3 cavern for long-lived exotics". In: *Physical Review D* 99 (1 Oct. 2018). DOI: 10.1103/PhysRevD.99.015023. URL: http://arxiv.org/abs/1810.03636%20http://dx.doi.org/10.1103/PhysRevD.99.015023.

[44] Giulio Aielli et al. "Expression of Interest for the CODEX-b Detector". In: *European Physical Journal C* 80 (12 Nov. 2019). DOI: 10.1140/epjc/s10052-020-08711-3. URL: http://arxiv.org/abs/1911.00481.

[45] CMS Collaboration. "Search for long-lived particles decaying in the CMS endcap muon detectors in proton-proton collisions at $\sqrt{s} = 13$ TeV". In: *Physical Review Letters* 127 (26 July 2021). DOI: 10.1103/PhysRevLett.127.261804. URL: http://arxiv.org/abs/2107.04838.

[46] ATLAS Collaboration. "Search for light long-lived neutral particles from Higgs boson decays via vector-boson-fusion production from pp collisions at $\sqrt{\{s\}} = 13$ TeV with the ATLAS detector". In: (Nov. 2023). URL: https://arxiv.org/abs/2311.18298v1.

[47] ATLAS Collaboration. "Search for light long-lived particles in pp collisions at $\sqrt{s} = 13$ TeV using displaced vertices in the ATLAS inner detector". In: (Mar. 2024). URL: https://arxiv.org/abs/2403.15332v1.

[48] Martin Bauer et al. "ANUBIS: Proposal to search for long-lived neutral particles in CERN service shafts". In: (Sept. 2019). URL: https://arxiv.org/abs/1909.13022v2.

[49] Demos Kazanas et al. "Supernova Bounds on the Dark Photon Using its Electromagnetic Decay". In: *Nuclear Physics B* 890 (Oct. 2014), pp. 17–29. DOI: 10.1016/j.nuclphysb.2014.11.009. URL: http://arxiv.org/abs/1410.0221.

[50] Jae Hyeok Chang, Rouven Essig, and Samuel D. McDermott. "Revisiting Supernova 1987A Constraints on Dark Photons". In: *Journal of High Energy Physics* 2017 (1 Nov. 2016). DOI: 10.1007/JHEP01(2017)107. URL: http://arxiv.org/abs/1611.03864.

[51] Yu-Dai Tsai, Patrick deNiverville, and Ming Xiong Liu. "The High-Energy Frontier of the Intensity Frontier: Closing the Dark Photon, Inelastic Dark Matter, and Muon g-2 Windows". In: *Physical Review Letters* 126 (18 Aug. 2019). DOI: 10.1103/PhysRevLett.126.181801. URL: http://arxiv.org/abs/1908.07525.

[52] Sarah Andreas, Carsten Niebuhr, and Andreas Ringwald. "New Limits on Hidden Photons from Past Electron Beam Dumps". In: *Physical Review D - Particles, Fields, Gravitation and Cosmology* 86 (9 Sept. 2012). DOI: 10.1103/PhysRevD.86.095019. URL: http://arxiv.org/abs/1209.6083.

[53] SHiP Collaboration et al. "Sensitivity of the SHiP experiment to dark photons decaying to a pair of charged particles". In: *European Physical Journal C* 81 (5 Nov. 2020). DOI: 10.1140/epjc/s10052-021-09224-3. URL: http://arxiv.org/abs/2011.05115.